https://ntrs.nasa.gov/search.jsp?R=19970018037 2020-06-16T01:54:52+00:00Z

NASA-CR-204438

INTERIM
IN-43-CR
OCIT
007779

Annual report for NASA grant NAGW-1110: Satellite Sensed Skin Sea Surface Temperature

Craig Donlon *Aerospace Engineering Science; Colorado Center for Astrodynamics Research (CCAR), Boulder, CO80302. Tel: (303) 492 0955 E-mail:cjdn@colorado.edu*

1 Introduction

Quantitive predictions of spatial and temporal changes the global climate rely heavily on the use of computer models. Unfortunately, such models cannot provide the basis for climate prediction because key physical processes are inadequately treated. Consequently, fine tuning procedures are often used to optimize the fit between model output and observational data and the validation of climate models using observations is essential if model based predictions of climate change are to be treated with any degree of confidence.

Satellite sea surface temperature (SST) observations provide high spatial and temporal resolution data which is extremely well suited to the initialization, definition of boundary conditions and, validation of climate models. In the case of coupled ocean-atmosphere models, the SST (or more correctly the "skin" SST (SSST)) is a fundamental diagnostic variable to consider in the validation process. Daily global SST maps derived from satellite sensors also provide adequate data for the detection of global patterns of change which, unlike any other SST data set, repeatedly extend into the southern hemisphere extra-tropical regions. Such data are essential to the success of the spatial "fingerprint" technique, which seeks to establish a north-south asymmetry where warming is suppressed in the high latitude Southern Ocean. Some estimates [*Allen,* 1993] suggest that there is a > 80% chance of directly detecting significant change (97.5 % confidence level) after 10-12 years of consistent global observations of mean sea surface temperature. However, these latter statements should be qualified with the assumption that a negligible drift in the observing system exists and that biases between individual instruments required to derive a long term data set are small. Given that current estimates for the magnitude of global warming of 0.015 K yr^{-1} - 0.025 K yr^{-1} [*IPCC,* 1995], satellite SST data sets need to be both accurate and stable if such a warming trend is to be

confidently detected.
This report describes the activities undertaken at the Colorado Center for Astrodynamics Research (CCAR) under research grant NAGW-1110: Satellite Sensed Skin Sea Surface Temperature. Some of these activities are focussed to develop and deploy instrumentation suitable for the collection of precise in situ measurements of the SSST which can be used to improve the accuracy of satellite measurements, while others develop techniques to generate improved global analyses of sea surface temperature using historical data.

2 The Effect of ΔT on the Accuracy of Satellite Derived SST Maps

Satellite SSST maps are now readily available from the precisely calibrated ERS-1 and -2 along track scanning radiometer (ATSR), and in the near future from the advanced ATSR (AATSR) and the moderate resolution imaging Spectroradiometer (MODIS) systems. Such infrared radiometers measure the sea surface temperature (SST) from a thin "skin" surface layer, having a depth equal to the e-folding attenuation length of infrared radiation in seawater (at a wavelength of 10μm this equates to a depth of $\sim$10-20 μm). Subsurface bulk SST (BSST) measurements can be significantly decoupled from the skin SST (SSST) because of diurnal warming events in the daytime and the cool skin temperature deviation at night. Temperature variations > 1 K are typical of a diurnal warming events [e.g., *Yokoyama and Tanba,* 1991] and variations of the order ± 1 K are experienced in the thin skin layer [e.g., *Donlon and Robinson,* 1997a; *Kent et al.,* 1996; *Schlüssel et al.,* 1990]. Consequently, the accuracy of satellite SSST or pseudo-BSST algorithms derived and validated using BSST measurements will always be limited, regardless of the success to which the effect of the intervening atmosphere can be compensated for using current multi-view and multi-spectral techniques. BSST validation data are subject to the geophysical limit imposed by ΔT and the accuracy of satellite derived pseudo-BSST and SSST data are constrained not only to the rms value of the BSST-SSST temperature difference (typically ± 1.0 K), but also the cool bias of $\sim$0.35 K imposed to the satellite derived SSST.

2.1 High Wind Speed - Low ΔT Conditions

One type of approach to validate satellite SSST observations using BSST observations is to use only satellite and subsurface buoy BSST observations collected in high wind speed (> 10 m s^{-1}) conditions. In these cases, the wind induced turbulence at the air-sea interface dominates the heat exchange between ocean and atmosphere; surface renewal is extremely rapid and therefore the skin temperature deviation is both small and stable. Thus the BSST is directly comparable to a infrared satellite observation [*Donlon et al.,* 1997a]. Further, wind speeds > 4 m s^{-1} prevent the formation of a diurnal layer eliminating this daytime complicating feature.

Certain areas of the oceans such as the sub tropical high-pressure regions, the inter-tropical convergence zone, or the trade wind belts, are characterized by "typical" wind speed conditions which could be used as broad indicators for the magnitude of ΔT. As there is a growing need to integrate SST observations from different satellite systems designed to return both SSST and BSST, the clear sky high wind speed combination will enable satellite SSST and BSST data to be merged with confidence. In terms of the validation, cross-comparison and inter-comparison of satellite systems required to ensure non-biased SSST data sets to be constructed for use in global climate studies [*Allen et al.,* 1994], these conditions are also preferred because more robust traditional BSST measurements can be compared to satellite data with confidence. This is an important point to consider in the context of the NOAA advanced very high resolution radiometer (AVHRR) which has been traditionally calibrated using BSST observations from drifting buoys. The high wind speed, negligible ΔT combination provide the mechanism to retrospectively calibrate AVHRR data to retrieve SSST and to reliable inter-calibrate individual satellite instruments.

In order to investigate this technique a pilot study has begun which compares global AVHRR GAC SSST observations to in situ NCEP drifting buoy data. The buoy data came from two sources: one was the Tropical Ocean Global Atmosphere (TOGA) buoys called the TOGA Atmosphere-Ocean (TAO) array. These data had been quality controlled and checked by the TAO office and the final results were available over the world wide web (WWW). The other buoy data were transmitted over the Global Telecommunication System (GTS) and are part of the NOAA's Coastal Environment Program (NCEP) Real-time Marine Observations and made available by Scott Woodruff of NOAA's Environmental Research Lab in Boulder, Colorado.

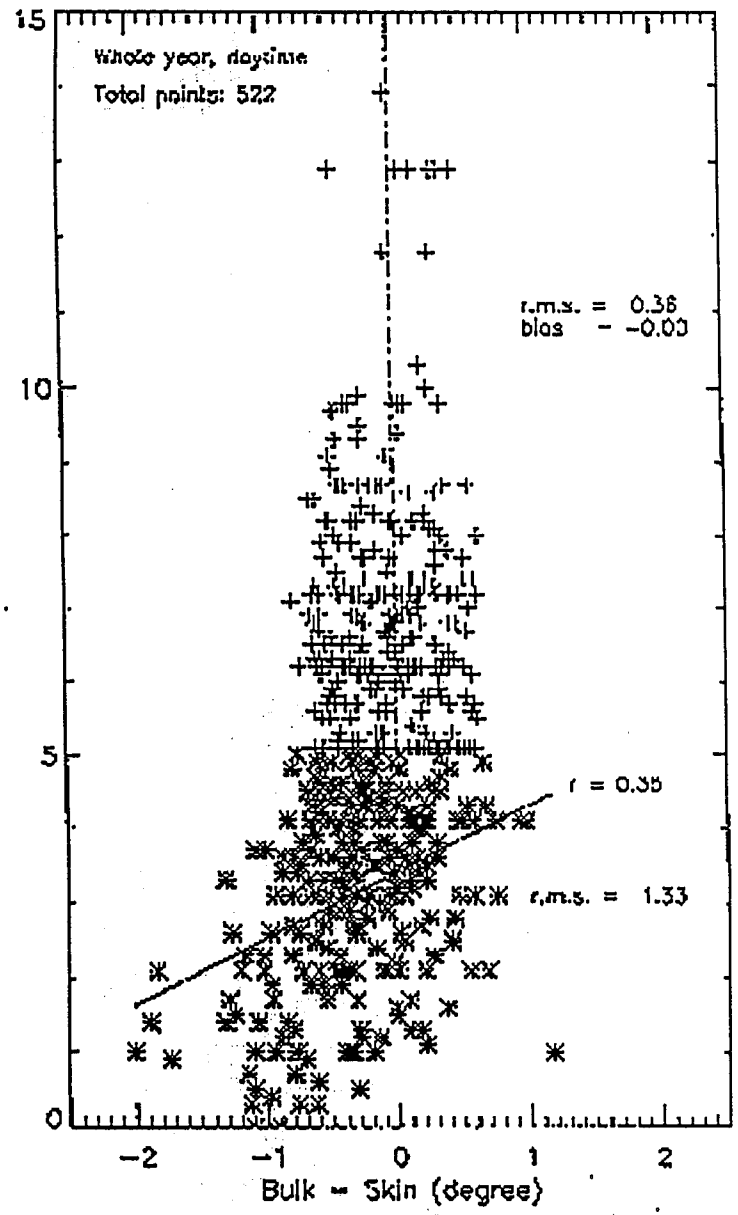

Fig. 1b. All seasons daytime buoy wind speed versus bulk-skin SST difference (ΔT).

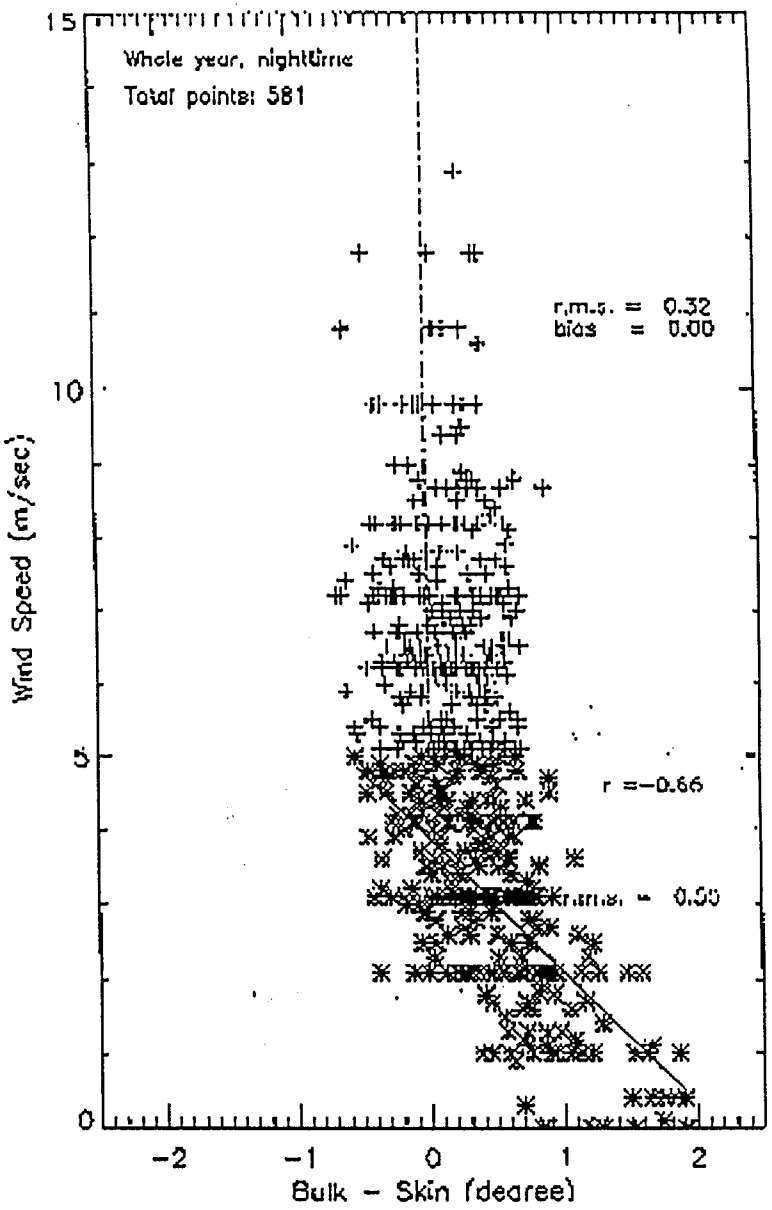

Fig. 1a. All seasons nighttime buoy wind speed versus bulk-skin SST difference (ΔT).

After the filtering and processing of both the buoy and the AVHRR/GAC data we plotted the relationship between ΔT and wind speed as a scatter diagram. All of the nighttime data are plotted here in Fig. 1a with a regression line fit to the points between 0 and 5 m/s. As expected there is a moderate negative correlation between ΔT and wind speed. This is consistent with the view that under neutral conditions the skin SST is lower than the bulk SST which leads to the concept of the "cool skin" of the ocean. Above 5 m/s this relationship between wind speed and ΔT changes to scatter about 0.0 K with an RMS value of 0.33 K. Switching to daytime (Fig. 1b) we see that below 5 m/s the slope of the line is now positive with most of the ΔT values being negative. In this case we can have an apparent "warm skin" which can occur when solar heating creates a diurnal mixed layer and the net difference between the skin and the deeper bulk temperature becomes negative. The correlation for this regression line is much weaker than the negative might-time correlation. In addition the RMS difference from the line was more than double the value for the nighttime conditions. Above 5 m/s the points again scatter about the 0.0 K line. The RMS of the ΔT values from this line is 0.35 K which is slightly greater than the 0.33 K RMS found for the overall nighttime comparison.

It is surprising how well the buoy and satellite data confirm aspects of the relationship between the skin and bulk SSTs [*Wick,* 1995) as derived from research measurements. We have extended these skin, bulk SST concepts to the study of routine measurements from moored buoys and infrared satellite sensors. The consistency of these results is clear evidence of the importance of the skin, bulk SST formation mechanisms. Furthermore the consistency between seasons for a large geographic area strongly suggests that these characteristics of the bulk-skin SST relationship hold true for all locations and seasons. These fundamental relationships are:

1. At wind speeds less than 5 m/s there is a moderate negative correlation between (bulk - skin) and the coincident wind speed for nighttime conditions. This indicates that the skin and bulk SSTs become similar as the wind increases to 5 m/s. At weaker winds (and indeed at calm conditions) the difference between bulk and skin SST are at their maximum reaching T values as large are 1.8 K (cool skin).
2. During the day solar heating creates "warm skin" conditions when a thin diurnal layer is setup that causes the skin SST to be higher than the bulk SST measured below this diurnal layer. Thus the correlation between wind speed and ΔT is positive and weak due to the increased scatter from the variable daytime conditions.

3. Above 5 m/s the line bisecting the distribution of K values is vertical about zero and the RMS deviation from this line is 0.35 K regardless of season. This is much smaller than any of the RMS values for the regression lines for the lower wind speeds.
These data have been presented at several conferences (see publications list below). This work has now been extended to include global AVHRR/NCEP data from 1992. We will also use the SSM/I sensor to derive wind speed estimates which then enables us to include more NCEP observations in the analyses.

3 The need for in situ Observations of ΔT

Unfortunately high wind speed conditions do not prevail across the global ocean and in situ radiometer measurements coincident in space and time with satellite observations are still required to validate satellite derived SSST. The widespread use of in situ research instrumentation such as the scanning infrared sea surface temperature radiometer (SISTeR) [*Nightingale,* 1997] or the modified-atmospheric emitted radiance interferometer (M-AERI) [*Smith et al.,* 1997, *Rivercombe et al.,* 1993] is limited both financially and practically. Thus, there is a need to explore different strategies for the on-going validation and calibration of satellite derived SSST and pseudo-BSST data sets as discussed by *Thomas and Turner* [1995]. Dr. Donlon participated in a trans Atlantic research cruise during September-October 1996 acting as Principal Investigator for the ROSSA 1996 experiment. A full cruise report is enclosed in Appendix A which describes the measurements made during this experiment. These data will be used to validate AVHRR and ATSR satellite measurements and as a large scale ocean Basin data set suitable for the further refinement and development of ΔT parameterizations. This type of data set provides much needed high quality measurements of not only ΔT , but also of the atmosphere ocean forcing terms (wind speed, temperature, radiation and humidity) required to fully investigate the complex and intimate relationship that exists between the bulk and skin SST. They do not, however, yield a comprehensive suite of measurements that can be used to calibrate-validate the infrared measurements made from space. For that we need measurements that are repeated on a regular basis over the same geographical region. Only a ship-of-opportunity program can satisfy this requirement. Bearing this in mind, the 1996 ROSSA experiment trialed several solid state infrared radiometer systems for use in

a ship of opportunity radiometer system. These results are fully reported in a recently submitted paper [*Donlon et al,* 1997d]. Based on these data, we propose to build and validate a new radiometer package which is described below.

3.1 The Ship of Opportunity Sea Surface Temperature Radiometer (SOSSTR)

The TASCO THI-500L radiometers have been extensively validated for the accurate determination of SSST both in the laboratory and in the field by many groups as thoroughly reported by *Donlon et al,* [1997d]. Repeated laboratory calibrations against a Committee of Action for the Study of the Ocean's Thermal Skin (CASOTS) precision blackbody unit [*Donlon et al.,* 1997c] were made in environmental chambers simulating a broad range of instrument temperature (278 - 305 K) as part of the CASOTS experiment. These experiments clearly show that the TASCO THI-500L radiometer is capable of maintaining a calibration of ± 0.1 K. Inter-comparison with simultaneous SSST observations made by a scanning infrared sea surface temperature radiometer (SISTeR) [*Nightingale,* 1997] made on different cruises highlight the excellent performance of the TASCO radiometers in the harsh conditions typical of ship installations.

However, these experiments highlight the need to adequately protect the radiometers form contamination by salt water, intense solar radiation and rain. The design presented here builds on an initial design developed by Southampton University, UK, which was successfully used during an experiment in the English Channel (see *Donlon et al.,* 1997a for a description). Figure 2 shows skin SST (SSST) determined from a typical deployment of the SOOSR instrument as a function of SISTeR SSST. The low rms and bias differences between the SOSSTR and SISTeR radiometers demonstrate that that reliable SSST measurements can be derived from the TASCO THI-500L radiometer systems. Deviations in this plot are due to temporal sampling differences and sea surface microlayes modifying the emissivity of sea water in the coastal regions (the cool temperature data). As the proposed system is to be operated autonomously, an independent reference blackbody is also required to monitor changes in the instrument calibration, which in this case, will be due primarily to contamination of the instrument fore-optics.

The SOSSTR radiometer package simultaneously measures the brightness temperature (BT) of the sea surface and of the atmosphere in the 8-12μm spectral window using two TASCO THI-500L infrared radiometer systems. The

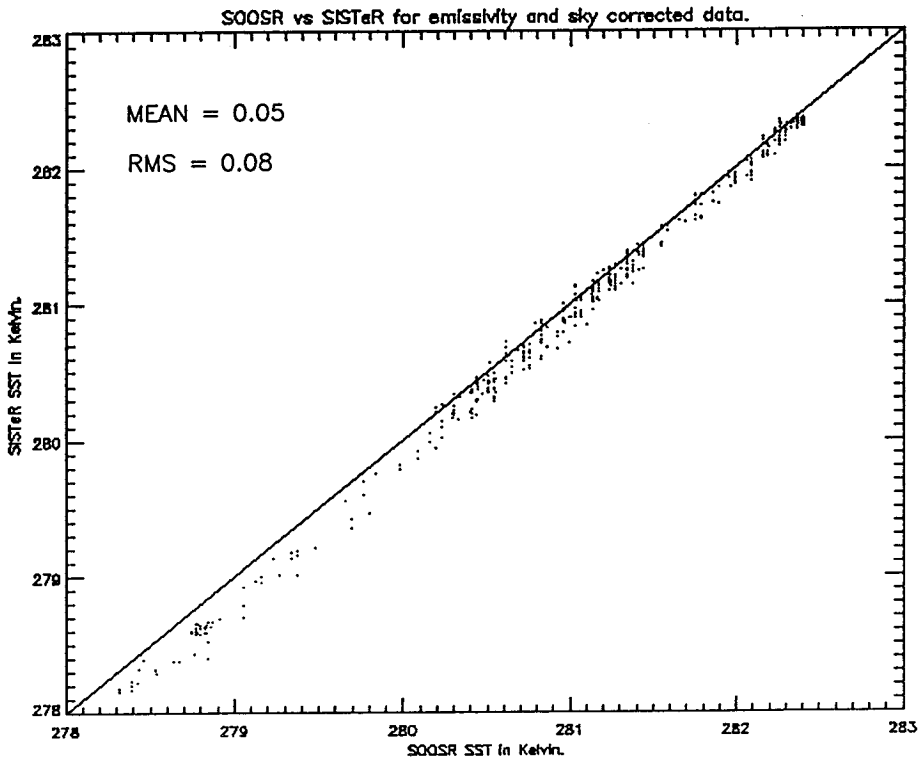
SOOSR vs SISTeR for emissivity and sky corrected data.
MEAN = 0.05
RMS = 0.08
SISTeR SST in Kelvin
SOOSR SST in Kelvin
283
282
281
280
279
278
278
279
280
281
282
283

Figure 2.

radiometers are mounted inside a rugged enclosure together with a dual blackbody calibration which is regularly viewed by each radiometer. The enclosure is maintained at a positive pressure to prevent contamination of the radiometer fore-optics by water ingress through a single aperture which is used by both instruments. The aperture is designed so that any water on the SOSSTR case will tend to flow away from the aperture. Data from each radiometer, the temperature of the calibration blackbodies and enclosure, are logged to a PC via a Campbell Scientific CR10X data logger interface. The link between logger and PC is digital, using short haul modems to minimize interference characteristic of the ship environment. Figure 3 provides a schematic diagram showing the layout of the SOSSTR instrument.

The geometry of the installation can be user defined to suit a particular installation using the specialized radiometer mountings which allow for view angles ranging from 15-50 degrees which can be verified using a small laser pointer (required to drastically simplify the installation and basic optical set up of the SOSSTR radiometer). Look angle in excess of this are not considered due to the difficulty of determining an appropriate value for the emissivity of sea water [Watts et al., 1996].

The blackbody used in this design is shown in Figure 4 and adheres to the basic guidelines described by *Berry,* [1981] and drawing on the experience of the Rutherford Appleton Laboratory, UK,. One unit will remain at an ambient temperature and a second will be heated to a nominal 10 K above ambient following a similar design to the RAL SISTeR radiometer. Using two independent blackbody sources an accurate measure of the system gain and offset can be made. To insure that this system does not degrade over time, the SOSSTR TASCO instruments will be independently calibrated at monthly intervals using a CASOTS blackbody [*Donlon et al,* 1997c]. This will ensure that the SOSSTR radiometer SSST remains accurate to 0.05 K. Simultaneous measurements of the BSST will be made using accurate thermistors attached to the ships hull. This is one of the most efficient methods of measuring BSST from a ship [Emery et al., 1997]. Sensors will be attached to the ship's hull at various depths below the sea surface because merchant ships, during the course of normal operations, the waterline depth changes as the ship is loaded and unloaded. Accurate thermistors are very cost effective and make it possible to install a vertical series of thermistors so that at least one of the units is below the waterline at all times. Time series of hull BSST coincident with ship injection temperatures show how the hull BSST response to changes in BSST is much faster than the injection temperatures which are found to lag BSST changes. Hull thermistors will be

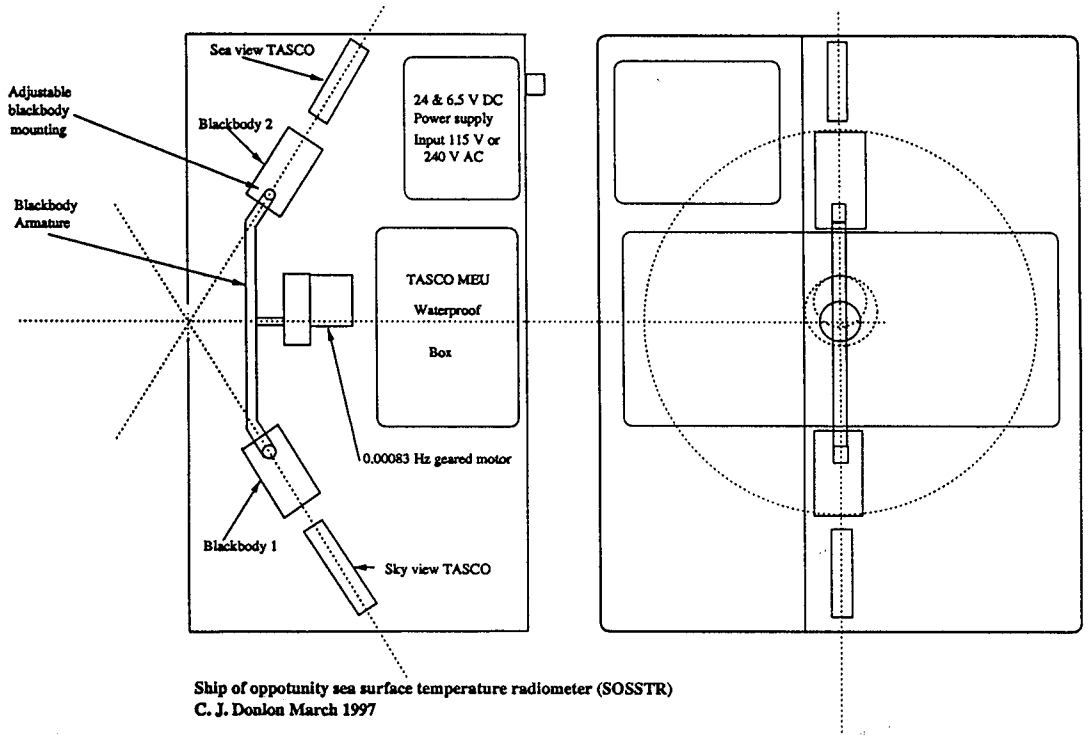

Ship of oppotunity sea surface temperature radiometer (SOSSTR)
C. J. Donlon March 1997

Figure 3

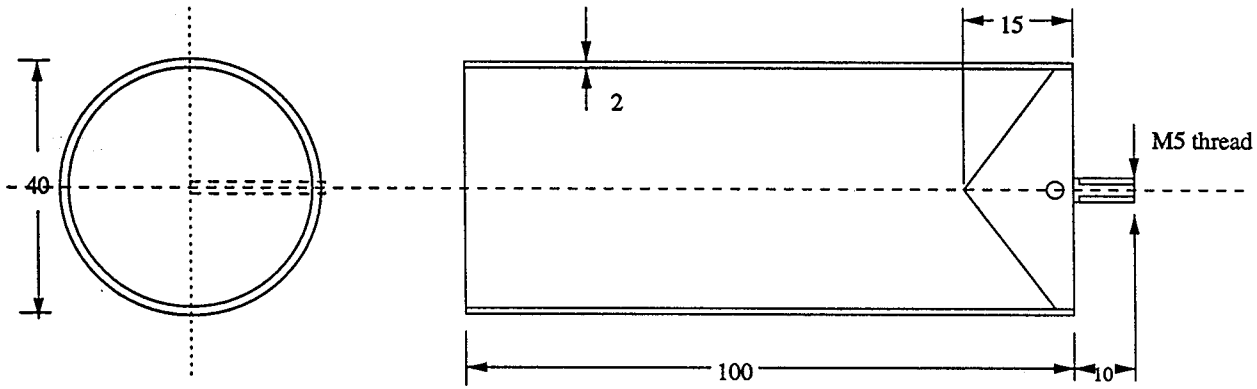

SOSSTR black body Mk.2 C J Donlon CCAR 1997

All material Alluminium

Figure 4.

logged to the Campbell Scientific CR10 coincident with the radiometer measurements described above. This system will be trialed during the MUBEX 1997 experiment, Mutsu Bay, Aomori, Japan in July 1997 in preparation for a more extensive trans Atlantic deployment during September-October 1997.

4 conclusion

Unfortunately, the processes controlling ΔT are complex and require further extensive characterization. At present the poor understanding of both ΔT and in situ SSST validation measurements are limiting factors when calibrating and validating satellite SSST and define the current geophysical limit to the accurate validation and calibration of satellite SSST and pseudo-BSST measurements. This highlights the need for a concerted international effort to collect further validation data for use in calibration and validation of infrared satellite observations. Improved ship borne radiometer systems are required together with a unified approach to the calibration of such instrumentation if ΔT is to be better characterized. It is clear that further studies of ΔT are essential if long term synergistic satellite data sets of SSST are not to be compromised by the intricate relationships that exist between the measured BSST and SSST during the validation process. The continued research activities undertaken at CCAR are striving to improve satellite derived sea surface temperature by developing new instrumentation and analyzing historical data sets which will produce an accurate and robust satellite sea surface temperature product.

5 References

Allen, M. R., C. T. Mutlow, G. M. C. Blumberg, J. R. Christy, R. T. McNilder, and D. T. Llewellyn-Jones., Global Change Detection, *Nature, 370,* 24-25, 1994.

Berry, T. H., Emissivity of a cylindrical black-body cavity with a re-entrant cone end face, *J. Phys. E: Sci. Instrum. 14,* 629-632, 1981.

Donlon, C. J. and I. S. Robinson., Observations of the oceanic thermal skin in the Atlantic ocean, *J. Geopys. Res., in press,* 1997 a.

Donlon, C. J. and I. S. Robinson., Radiometric validation of the ERS-1 ATSR average sea surface temperature in the Atlantic Ocean, *Submitted to the J. Atmos. and Ocean. Tech.,* 1997 b.

Donlon, C. J., T. J. Nightingale, L. Fielder and I.S.Robinson., A low cost blackbody for the calibration of sea going infrared radiometer systems, *Submitted to the J. Atmos. and Ocean. Tech.,* 1997 c.

Donlon, C.J., S. J. Keogh, D. J. Baldwin, I. S. Robinson, I. Ridley, T. Sheasby, I. Barton, F. Bradley, T. Nightingale, and W. Emery, Solid state radiometer measurements of sea surface skin temperature, *Submitted to the J. Atmos. and Ocean. Tech.,* 1997d.

Donlon, C. J., *Radiometric Observations of the Sea Surface and Atmosphere: 1996 cruise report,* University of Colorado, Boulder, CCAR internal report, 1997 d.

Kent, E. T., T. Forrrester and P. K. Taylor, A comparison of the oceanic skin effect parameterisations using ship-borne radiometer data, *J. Geophys. Res., 16,* 649-16,666, 1996.

Nightingale, T. J., *The scanning infrared sea surface temperature radiometer (SISTeR),* RAL internal report, Rutherford Appleton Laboratory, Chilton, Didcot, Oxon., England, 1997.

Rivercombe, H. E., F. A. Best, R. G. Dedecker, T. P. Dirkx, R. A. Herbsleb, R. O. Knutesen, J. F. Short, and W. L. Smith,*Atmospheric Emitted Radiance Interferiometer for ARM. Symposium on Global change Studies.*, January 17-22,1993.

Schlüssel, P., Emery, W. J., Grassl, H. and Mammen, T., On the Bulk Skin Temperature Difference and its Impact on Satellite Remote Sensing of Sea Surface Temperature. *J. Geopys. Res., 95,* 13,341-13,356, 1990.

Smith W. L., R. O. Knuteson, H. E. Rivercomb, W. Feltz, H. B. Howell, O. Brown, J. Brown, P. Minnett, W. McKeown, Observations of the Infrared radiative properties of the ocean - Implications for the measurement of sea surface temperature via satellite remote sensing, *Submitted to Bull. Am. Met. Soc.,* 1997.

Thomas, J. P. and J. Turner, Validation of Atlantic Ocean surface Temperatures Measured by the ERS-1 Along Track Scanning Radiometer, *J. Atmos. and Oceanic. Tech., 12,* 1303 - 1312, 1995.

Watts, P. D., M. R. Allen, and T. J. Nightingale., Wind speed effects on sea surface emission and reflection for the Along Track Scanning Radiometer, *J. Atmos and Oceanic Tech., 13,*, 126-141, 1996.

Yokoyama, R. and S. Tanba., Estimation of sea surface temperature via AVHRR of NOAA-9 –Comparison with fixed buoy data, *Int. J. Rem. Sens., 12,* 2513-2528, 1991.

6 Publications submitted under this grant

Donlon, C. J. and I. S. Robinson, Observations of the oceanic thermal skin in the Atlantic ocean, In press J. Geophys. Res., 1997.
Donlon, C. J. and I. S. Robinson., Radiometric validation of the ERS-1 ATSR average sea surface temperature in the Atlantic Ocean, Submitted to the J. Atmos. and Ocean. Tech., 1997.
Donlon, C. J., T. J. Nightingale, L. Fielder and I.S.Robinson., A low cost blackbody for the calibration of sea going infrared radiometer systems, Submitted to the J. Atmos. and Ocean. Tech., 1997.
Donlon, C. J., S. J. Keogh, D. J. Baldwin,I. S. Robinson,I. Ridley, T. Sheasby, I. Barton, F. Bradley, T. Nightingale and W. Emery., Solid state radiometer measurements of sea surface skin temperature, Submitted to the J. Atmos. and Ocean. Tech., 1997.
Donlon, C. J., Validation of the ERS-1 ATSR Average Sea Surface Temperature product in the Atlantic Ocean, (abstract), Eos Trans. AGU, 77(46), Fall meet. suppl., 1997.
Emery, W. J, C. J. Donlon, and I. S. Robinson., Wind speed forcing of the bulk-skin sea surface skin temperature difference, (abstract), Eos Trans. AGU, 77(46), Fall meet. suppl., 342, 1997.
Parkes, I., T. Sheasby, D. L:lewwellyn-Jones, C. T. Mutlow, T. Nightingale, A. Zavody, R. Yokoyama, S. Tanba, C. J. Donlon, The Mutsu Bay Experiment: An investigation into the Physical Processes of the Ocean-Atmosphere Boundary Unibg ATSR data and in situ measurements, Third

ERS Symposium, Florence, Italy, 17-21, March 1997.

7 Appendix A. Rossa 1996 Cruise Report

Radiometric Observations of the Sea Surface and Atmosphere: 1996 cruise report.

C J Donlon*

December 12, 1996

Abstract

This report describes the scientific activities undertaken during the Radiometric Observations of the Sea Surface and Atmosphere (ROSSA) 1996 experiment aboard the RRS *James Clark Ross* while on passage from the UK to the Falkland Islands, 19th September 1996 - 21st October 1996. The primary objective of ROSSA is to further current understanding of the exchange of heat and momentum at the air sea interface by collecting detailed oceanographic and meteorological observations of the sea surface and overlying atmosphere using both satellite and shipboard measurements. 5 infra-red radiometer systems were deployed during the experiment which were calibrated using a CASOTS precision black body calibration target. A comprehensive suite of ocean - atmosphere variables were also measured in order to investigate their complex relationships to the bulk - skin temperature deviation ΔT . Collaboration with the Atlantic Meridional Transect (AMT-3) experiment (also on board the ship) investigated the differences between radiometric SST and traditional bulk SST corrections when applied to temperature soluble gases such as CO_2 using direct measurements of bulk and skin sea surface temperature. This report describes the instrumentation deployed and the basic data sets generated during the ROSSA 1996 experiment and the relevant data sets collected by the AMT-3 experiment which will be used by ROSSA 1996.

*Colorado Center for Astrodynamics Research, Boulder, Colorado

1 Introduction

The transfer of heat across the atmosphere-ocean interface is fundamental to the prediction of climate and a through understanding of this process is vital to the successful coupling of ocean - atmosphere models [Hadley center, 1994] because sea surface temperature (SST) influences the exchange of heat, momentum, moisture and gases across the air sea interface [e.g. Robinson et al, 1985]. Global sea surface temperature is routinely measured by several satellite infrared radiometer systems and the frequent, large spatial sampling capability of satellite instruments generates data sets suitable for the direct detection of global climate change using a variety of techniques [Allen et al, 1994]. However, as infrared radiometer systems give an estimate of the SST from an infra-red optical depth (optical depth is in this case the e folding attenuation distance of infrared radiation in sea water) of between 40 - 60 μm, the derived SST measurement is a 'skin' temperature or SSST. Although having an extremely small depth it is the SSST layer that not only controls all exchange of heat and momentum between the atmosphere and ocean and but also the exchange of temperature soluble gases such as CO_2 [Hasse and Liss, 1981; Robertson and Watson, 1992; Van scoy et al, 1995 Stephens et al, 1995]. The SSST is typically 0.3 - 0.5 K cooler [e.g. Coppin et al, 1991; Schluessel et al, 1990] than the water immediately beneath (which is referred to as the bulk SST or BSST). Extreme skin temperature deviations, (ΔT , defined here as the bulk temperature - skin temperature) of greater than about $\pm$ 1.0 K have been reported [Donlon and Robinson, 1996] and a ΔT reformation time scale of the order 10 seconds has been quoted [Jessup, 1992] based on thermal images of the sea surface after the surface water has been disturbed. Now that a new generation of satellite radiometer systems such as the ERS Along Track Scanning Radiometer (ATSR) [Edwards et al, 1990] are now capable of achieving a SSST precision to better than 0.3 K [Mutlow et al, 1994] (within the extreme magnitude expected for ΔT), it is no longer acceptable to ignore the difference between the SSST measured by satellite infrared radiometers and the BSST conventionally measured by ships and buoys in the upper 1 - 10 m of the water column. If accurately validated non-biased satellite SST observations are available for a 10 year period there is a ¿80

In order to address some of the issues discussed above the a team led by the British Antarctic Survey (BAS) in collaboration with the Colorado Center for Astrodynamics Research (CCAR), the Rutherford Appleton Laboratory (RAL), the National Aeronautics and Space Administration (NASA),

Southampton Oceanography Center (SOC) and National Space Development Agency of Japan (NASDA) have made a series of atmospheric and oceanic measurements along a transect from the UK to the Falkland Islands. Figure 1 shows the ship track made by the RRS *James Clark Ross* (JCR) on her southerly passage from the UK to the Falkland islands made during the period 20th September - 20th October 1996. The ROSSA 1996 field campaign deployed several new ship-mounted radiometer instruments and measured many of the key oceanographic and atmospheric variables thought to influence ΔT . The measurements collected provide an extremely comprehensive data set for the investigation of ΔT at both a regional and global scale. The specific objectives of the ROSSA 1996 experiment are as follows:

- To characterize the diurnal nature, variability and climatic regionality and seasonality of ΔT in the Atlantic ocean using measured precision ocean - atmosphere data set.
- To determine the relationship between the radiometric SSST and the subsurface BSST measured at depths ranging from 0.1 - 100 m by measuring sufficient atmosphere - ocean parameters to fully specify the processes governing this relationship.
- To derive and validate a set of algorithms suitable for the conversion of SSST to BSST applicable at a global scale using *in-situ* observations coupled to 1 dimensional model fields of diurnal warming in the upper layers of the ocean.
- To asses the importance of ΔT for climate studies of heat exchange between the atmosphere and ocean in a number of different climatic regions.
- To investigate techniques for the validation of infrared satellite observations of sea surface temperature derived from several satellite instruments and to develop algorithms for the synergistic use of such data sets to produce high quality non biased estimates of both SSST and BSST.
- To determine the importance of using SSST rather than BSST when investigating the atmosphere - ocean exchange of temperature soluble gasses such as CO_2

ROSSA 1996 collaborated with the Atlantic Meridional Transect experiment 3 (AMT-3) which operated in parallel with ROSSA 1996 aboard the

Parameter	Instrument	Accuracy	Precision	Height
SSST	RAL SISTeR	0.05 K	0.05 K	16.5 m
SSST	MISTRC	0.1 K	0.1 K	7m
SSST	TASCO THI-500	0.5 K	0.1 K	16.5 m
SSST	KEYENCE IT2-60	0.1 K	0.1 K	22 m
SSST	TH3100	0.1	0.1	22 m
IR sky T°	RAL SISTeR	0.05 K	0.05 K	16.5 m
IR sky T°	TASCO THI-500	0.5 K	0.1 K	16.5 m
BSST	Trailing PRT	0.02 K	0.02 K	-0.1 m
BSST	Hull thermistor	0.1 K	0.1K	-2.5 m
BSST	SeaBird TSG	0.005 K	0.001 K	- 5.5 m
BSST	CTD	0.005 K	0.001 K	-1 to -100 m
BSST	XBT	0.1 K	0.5 K	-5 to -2000 m
Dry bulb T°	PRT	0.002 K	0.005 K	16 m
Wet bulb T°	PRT	0.002 K	0.005 K	16 m
Solar radiation	CM-5 Solarimeter	1 W/m2	1 W/m2	16 m
Solar radiation	CM-5 Solarimeter	1 W/m2	1 W/m2	26 m
LW radiation	Eppley Pygeometer			26 m
Wind speed	Sonic Anemometer	0.1 m/s	0.1 m/s	26 m
Wind direction	Sonic Anemometer	5°	1°	26 m
Sea surface roughness	X band radar			16 m

Table 1: Summary of the measurements made during ROSSA 1996 September - October 1996.

JCR. This collaboration was especially important for ROSSA 1996 due to the gas exchange, XBT, UOR and CTD measurements being made which will be used in conjunction with the radiometric observations made as part of ROSSA.

2 Instrumentation

Table 1 describes the instrumentation that was fitted to the JCR during the 1996 ROSSA experiment and the following sections describe the individual systems used together with a summary of their deployment, operation and problems encountered during the experiment.

2.1 SSST - Radiometrically determined sea surface skin temperature.

Five radiometer systems were deployed during the ROSSA 1996 experiment in order to assess the effect of different calibration schemes and because the measurements made were somewhat different in character. For instance the thermal infrared camera system was used to determine a 2 dimensional SSST image measurement whereas all of the other radiometer systems simply return a spot measurement. Of particular interest was the use of inexpensive 'solid state' hand held radiometer systems such as the TASCO TH-500 and Keyence IT2-60 devices. By developing such instrumentation during the ROSSA experiments it is hoped that an inexpensive autonomous ship of opportunity radiometer package can be developed suitable for the widespread calibration and validation of satellite SSST measurements. Each of the radiometer systems used during ROSSA 1996 is discussed below.

(a) Scanning Infra-red Sea surface Temperature Radiometer - SISTeR (T. Nightingale, RAL) This is a multispectral scanning ship-mounted infrared radiometer designed to measure the SSST with an accuracy approaching 0.05 K. The SISTeR is a self-calibrated radiometer, relying on two precision black body cavities maintained at different temperatures. The instrument can view any point in external swath extending up from a nadir (vertically downward) view, in addition to the two internal black bodies.

All aspects of the instrument, including the black body temperatures and the scan sequence, are fully controllable from a simple "C" program, allowing users to adopt different sampling strategies depending on their requirements. For the AMT-3 cruise, one black body was operated at the ambient temperature of the instrument and the second at $\sim$ 8K above ambient temperature. Table 2 summarizes the scan mirror cycle used during the ROSSA 1996 campaign. All data were collected over 0.8 second sample periods, using a single filter centered at $\sim 10.9\mu$m with a bandwidth of $\sim 0.8\mu$m.

Fugue 2 shows a 'typical' SISTeR signal data trace which has been annotated for clarity. Clearly seen is the hot black body warm up in the first 0.5 hours after deployment ($\sim 3.3 \times 10^4$ counts), the ambient black body having a temperature close to the sea surface ($\sim 3.2 \times 10^4$ counts) and the highly variable sky temperature signal. The smaller numbers in the sky temperature signal represent clear sky conditions ($\sim 2.8 \times 10^4$ counts) and the higher counts cloudy conditions (typically at 3.15×10^4 counts in this example). After some initial problems successful deployments commenced

Target	Samples
Move	8
Hot BB	8
Move	8
Sky	8
Move	8
Sea	24
Move	8
Cold BB	8
Move	8
Sky	8
Move	8
Sea	24

Table 2: SISTeR scan mirror cycle used during ROSSA 1996 September - October 1996.

on the 27th September and continued until October 23rd 1996 with breaks due to calibration experiments and poor weather conditions as shown in figure 3 and table 6. During periods of poor weather, the instrument was protected initially by a plastic bag which totally sealed the unit from water ingress. As access to the forward mast island was only possible during daylight hours, this meant that a decision whether to close down the instrument during the hours of darkness had to be made at around 6.00 PM local time each evening. In order to alleviate this problem, a manually operated door was manufactured which covered the instrument's entrance aperture and attached to the pre-drilled and tapped holes provided on the SISTeR case. The door could be opened or closed using cables run down the mast to the foredeck area. As the instrument is sealed apart from the entrance aperture, it could almost be totally protected in bad weather without requiring access to the forward mast island using the manufactured door. From the 8th to the 10th October, the instrument was de-rigged and brought into the laboratory for calibration using a CASOTS water bath black body unit. Initial inspection of the scan mirror showed that the aluminum mirror substrate had been attacked by the maritime environment, presumably through imperfections in the rhodium-plated surface. The scan mirror was replaced

with a spare unit, the instrument was realigned and re-calibrated and then reinstalled on the forward mast. The instrument then remained in place for the remainder of the voyage, except for a short interval on the 14th October, and again on the 21st October at Montevideo, when additional calibrations were undertaken.

When inspected at the end of the voyage, the second scan mirror also showed signs of corrosion. To first order, this corrosion does not have any significant effect on the overall calibration of the instrument, as the two internal calibration measurements made by the instrument are affected by the mirror degradation in the same way as the external measurements. This is a specific design feature of this instrument and an initial inspection of the calibration data confirms that significant calibration deterioration had not occured and that the instrument has measured the brightness temperature of the sea. An early example plot of typical output is shown in figure 4. In this figure, the radiometer measures a highly variable signal in the presence of a large internal wave field having large associated slick features during the period 5-10 hours.

(b) Multi-Channel Infrared Sea Truth Radiometric Calibrator - MISTRC. This is a dual head precision multi spectral radiometer system which uses a single variable temperature internal black body cavity together with a stirred tank of sea water to derive a SSST accuracy of better than 0.1 K. The calibration strategy used by this instrument is significantly different from the SISTeR system in that it does not require knowledge of the sea surface emissivity. Instead the temperature of the bath of sea water which is well stirred (at a temperature similar to the sea surface) is used as an absolute calibration source for the instrument. The difficulty with this technique is that the sea surface roughness and sky conditions are assumed to be uniform during the calibration and sea surface views the instrument requires. The MISTRC was deployed from the bow of the JCR using a specially designed mounting bracket which allowed the instrument to be quickly and easily brought in board during bad weather. This system worked extremely well and the instrument could be made safe in 2-3 minutes. This involved detaching the translation stage from the instrument table using quick release bolts and stowing the entire unit in a locker room, swinging the optical head inboard and lashing this down, capping all sockets on the MEU and securing the sea water plumbing system. However it should be pointed out that the MISTRC system is extremely cumbersome and difficult

to deploy due to the main electronics unit sitting in a large aluminum box (23 x 16 x31 inches), the requirement for sea water and large number of cables required to operate the instrument. Sea water was taken from the ships scientific pumped supply and led up to the bow region using plastic tubing. Although a spare booster pump was packed as part of the MISTRC system, it was not necessary to use this as the ships water pressure was sufficient to completely stir the calibration bucket. In fact the valves used to control the water flow to the bucket needed to be partly closed as the mixing was too intense and water was overflowing the bucket rim. Several modifications had been made to the bucket assembly itself before deployment to prevent both overflowing and ease the gimbal movement including the addition of a second drain port and lowering the center of balance. These modifications were insufficient to prevent the water bath from 'backing up' and listing to one side or the other thus allowing water to pour over the bucket side and splash the instrument via updrafts from the ships bow. It is recommended that future deployments of the MISTRC should use a completely redesigned bucket system as suggested by the last MISTRC cruise report.

Perhaps the greatest problem with this system is the effect of wind over the bucket picking up water and splashing the instrument fore-optic lenses. Once these become wet, the instrument will simply sense the temperature of the thin water film of the lens rather than the SSST. During the initial deployments of the instrument, a 2 hour watch was required 24 hours per day in order to keep the MISTRC lenses clean. At the very least a baffle arrangement for future deployments used in combination with a redesigned free draining bucket system will minimise splashing of the lenses. Unfortunately, the cabling between the radiometer head and the system electronics unit was corroded rendering the instrument unserviceable for the entire cruise. Most of the system was working perfectly (translation stage, sampling , and filter wheel) but the chopper motors would not spin up. Several attempts were made to repair the cable termination's which were 50 pin crimped and sealed military style connections, but as the appropriate tooling was unavailable this was unsuccessful. Consequently the instrument was de-rigged and stowed for the duration of the cruise.

(c). Ship Of Opportunity Sea surface temperature Radiometer - SOOSR (S Keogh, SOC). The SOOSR system comprises of two single channel broad band (8 - 12 μm) TASCO THI-500L radiometer units operated in tandem one set to view the sea surface and a second to view the sky in the source

region of directly reflected radiation at the sea surface. The TASCO instruments have been laboratory calibrated using CASOTS black body cavities to better than 0.2 K. Basic calibration is derived from an internal look-up-table programmed into the instrument by the manufacturer. However this calibration assumes that the radiometer fore optics remain uncontaminated by sea or rain water which was not the case during the ROSSA 1996 experiments. In order to minimize contamination, the TASCO instruments were housed in a large box which had a small aperture cut for the radiometers to view the sea and sky. A fan unit was then used to force air out of the aperture in an effort to prevent spray etc. contamination the lenses.

Problems arose during the mounting of the SOOSR instrument as the box used to house the radiometer units and forced air system was rather large. Eventually a suitable place was found on the JCR forward mast area using wooden wedges to prop up the housing. This was required so as the sky and sea view radiometers were not viewing any part of the ships superstructure (hand rails). Power was taken from the fore mast junction box supplying 240 v AC and data was logged to a Cambell Scientific CR-10 data logger located at the foot of the mast. This arrangement was chosen so that it was not necessary to climb the ships mast in order to download the TASCO data which was required twice daily due to the limitation of the data logger storage capacity. Future deployments should use the RhoPoint module system which is accessible from the ships mast to log all data to the ships Oceanlogger system. The instruments were set at a sample frequency of 5 seconds and logged at 20 second intervals using an emissivity value of 1.0 along the transects shown in figure 5 and in table 5. Unfortunately it appeared that the radiometers were viewing a part of the instrument housing as cooler SSST temperatures of between 1 and 2 K were recorded when the TASCO instruments were deployed *outside* of the SOOSR box.

In order to simplify the deployment, the radiometers were mounted directly to the ships rail. This resulted in significant contamination of the fore optics lenses at times although these were cleaned on a regular basis. Calibrations against the CASOTS black body made during the ROSSA 1996 experiment showed differences of > 3 K and a distinctly non-linear response curve when the fore optics were contaminated as shown in figure 6. Notice the small differences at and around the crossing point of the two curves which is the instrument (air) temperature. In this region the differences due to contamination are small of between 0.4 K - 0.6 K over a 3 K

range. In order to calibrate these data, environment variables such as the air - sea temperature difference together with the calibration data collected during ROSSA 1996 and the SISTeR data will be used to derive a robust calibration scheme for the TASCO radiometers. To ensure a high quality data set, the TASCO data will be cross calibrated with the SISTeR data and contaminated data removed from any further analysis. However this may prove difficult as the contaminated data will be only slightly different from the true calibration depending on the temperature of the fore optics train and the degree of contamination. Figure 7 shows an example of the raw TASCO data collected during the same time as that shown in figure 4. The top panel shows the sky temperature signal and the lower panel the sea surface signal. Comparing with figure 4, the reduced sample rate used by the SOOSR results in a significant loss of detail in both plots - notably the sky signal is very smooth indeed. However, the fact that a similar trace is seen in the SSST signals is encouraging and although the amount of detail is not as great in the SOOSR data as the SISTeR, the SOOSR instrument seems to perform well. Note that the offset between figure 4 and 7 is due to the preliminary analysis performed on the data sets assuming an emissivity for sea water of 0.98 for the SISTeR data and no analysis of the SOOSR data.

(d) Keyence IT2-60 (Y. Terrayama, NASDA). This is a similar solid state radiometer system to that of the TASCO discussed above which was deployed from the Port side top deck bridge wing using a view angle of 40° . Unlike the TASCO instruments which were essentially unattended during the majority of the ROSSA 1996 experiment, the Keyence radiometer was always used under supervision and thus the for optics were kept clean at all times. Calibrations were made using the CASOTS black body unit during the ROSSA experiment as shown in figure 8 which clearly demonstrate the benefit of having dedicated personnel present to protect the instrument from spray and rain. A useful feature of the Keyence radiometer was a laser sight system which aided both calibration and initial deployments of the instrument itself. As the spectral bandwidth is similar to that of the TASCO radiometers, any future SOOSR system should use Keyence radiometers as opposed to TASCO instruments.

(e) Thermal infrared camera - NEC THI3100 (Y. Terrayama, NASDA) A NEC THI3100 thermal infrared camera was deployed from the port side top deck bridge wing at a height of 20 m above the sea surface and a view

angle of 40° . In this configuration the camera was able to view the ships bow wave and unaffected clean water having a field of view covering approximately 20.8 x 10.24 m with a pixel size of 0.5 x 0.5 m. The camera uses a waveband of 8 - 13 μm and a cooled HgCdTe detector element digitized to 12 bits at an accuracy of 0.1 K and resolution of 0.025 K at 303 K. The sample integration time used during the ROSSA 1996 experiment was approximately 50 seconds. As this was the first time that such a device had been deployed from the RRS *James Clark Ross* there were significant installation problems to overcome. The main problem with the instrument was the lack of environmental protection which ultimately resulted in the filter window coating corroding away. Future deployments should provide adequate protection from salt water spray and rain water. Calibrations were performed against the CASOTS black body unit and these data are currently being processed.

2.2 BSST - subsurface sea surface temperature.

Although a continuous vertical temperature profile in the top 2 m of the water surface was desirable only several subsurface temperatures were continuously measured at different depths. Descrete temperature profiles were made only when the ship stopped on a daily station. The following instrumentation was used during ROSSA 1996:

(a) BSST at 0.1 m An IOS SOAP trailing thermistor unit was deployed from the port flank of the JCR a depth of $\sim$ 0.1 m. This depth is in accordance with the ΔT measurement strategies discussed at the first CASOTS (Combined action to study the ocean's thermal skin) workshop held at Southampton Oceanography Center, UK, June 1996. A 3 m scaffold pole was used to pole out the cable which initially used several weights attached over the length of the unit to sink the sensor. It was soon apparent that a significant weight was required and a large shackle was attached. This sunk the SOAP sensor to the required depth (0.1 -0.2 m while underway) and kept the sensor in the water. Unfortunately, the cable parted due to this weight due to the additional drag and 1 unit was lost. A second system was then developed using steel cable shackled at both ends to carry the large weights required to sink the sensor head. This system remained in operation for the remainder of the cruise although during periods when the ship speed exceeded 14 kt, the sensor head was not always in the water.

Consequently the instrument was brought inboard. Several re-terminations of the cable were required as the steel cable had shards which punctured the SOAP cable. These were executed on board with minimal disturbance to the sensor. Negligible resistance differences were found after the termination's were completed and the calibration of the SOAP remains viable. Temperature profiles were made as the instrument sunk once the ship had stopped on station. In this way, 2 temperature profiles were made at the beginning and end of each daily station to a depth of approximately 15 m.

This instrument was a major success as all data were logged to the ships computer system via RhoPoint module. It is highly recommended that any future system requiring logging is engineered to take advantage of the BAS Oceanlogger system. This system will take up to 13 additional inputs from sensors interfaced using RhoPoint modules. Software configuration allows a user defined log interval and label system to each additional parameter and will apply calibrations if required. All Oceanlogger data are seen as a single RVS Level B data stream easing the data logging and post processing task once up to a Level C process. The Oceanlogger system was designed, built and maintained by P. Woodruff (BAS ISG).

(b) BSST at 2.5 m. A hull mounted UKMO thermistor was used to determine BSST at 2.5 m. These data are pendig a detailed analysis using other underway temperature measurements due to a suspected calibration error.

(c) BSST at 5.5 m. The JCR has a 'Sea Bird' thermosalinograph unit having an extendible intake pipe located at a depth of 5.5 m and operated continuously for the entire cruise. Salinity samples were taken at regular intervals throughout the cruise for calibration purposes as were UKMO bucket SST measurements. Figure 9 plots a subsample of the entire ROSSA 1996 5.5m BSST measurements and clearly demonstrates the range of temperatures encountered during a passage such as this. Noticeable in this figure is the diurnal range of temperatures typically having a magnitude of $\sim$ 1K.

(d) BSST at 2.0 - 80.0 m (Jim Aiken, PML). A UOR (Undulating Oceanographic Recorder) measuring temperature and salinity was used to determine the BSST in the upper 80 m layer of the ocean. This instrument measures underway profiles of temperature and salinity reaching a maximum depth of 100 m and operating at a nominal maximum of 80 m. Typically the

instrument was towed at a speed of 11-12 kt using 370 m of cable resulting in an undulating depth amplitude of 5 - 66 m and an undulating pitch of 3 km. The UOR was generally towed after a mid morning station for 4 - 7 hours through the sunlit period of the day although two long overnight tows were made across the equatorial upwelling and before the Montevideo port call as shown in figure 10. These data are currently being processed as part of the AMT-3 experiement and will be available toi the ROSSA project in the near future.

(e) BSST at depths in excess of 100 m (Colin Griffiths, PML). Two daily Conductivity, Temperature and Depth (CTD) casts to a depth of 200 m were undertaken close to the local solar maximum using a Neil Brown Mk IIIb CTD. All data was logged via the ships internal system and reversing thermometer calibration data were taken at 7 m and 200m at each station. Expendable Bathythermograph (XBT) sondes (Sippican Mk. T5 to 1830 m and Sparton T7 to 760 m) were released at regular intervals with some increased casts in the Brazil - Falklands current convergence for satellite SST validation studies using the AVHRR as clear skies persisted. The T5 and T7 XBT's profile the deep ocean for temperature and pressure only which were logged to a Sippican Mk.9 data acquisition package. Post processing of all data was performed using the accompanying Sippican software.

2.3 Meteorological observations

Wind speed and direction were determined from a sonic anemometer system located at a height of 20 m in clean air on the JCR front mast instrument table. This instrument is part of the permanent scientific equipment maintained and operated by the JCR/ BAS teams and a subsample of the wind speed encountered during ROSSA 1996 is shown in figure 11. A large range of wind speed conditions were encountered during the ROSSA 1996 experiment ranging between 0 and 22 $ms^{-}1$ having peaks on Jday 268 and 291. Note the data break between Jday 292 and 295 for the Montevideo port call.

Long- and short-wave downwelling fluxes. Eppley pygeometer and pyranometer instruments measuring the direct downwelling long and short-wave fluxes were mounted on the dedicated upper radiometer platform of the JCR using custom gimball mounts. Data from these instruments was logged to a PC via a MAC-7 data acquisition system and were logged continuously throughout the cruise. A second solarimeter unit (Kipp and Zonen CM-5)

was mounted on the JCR forward mast hand rail and is part of the JCR / BAS fixed equipment. Figure 12 shows calibrated example plots derived from the CCAR Eppley pygeometer and solarimeter respectively covering a 3 day period.

Air temperature and humidity. An IOS WOCE standard psychrometer unit was used to measure air temperature and humidity from the forward mast of the JCR. This was attached to a stub pole to clear the intake area from the forward mast upper island deck which may convectively influence the PRT sensors when the deck is hot. These data were logged to the ships Oceanlogger system via RhoPoint modules located on the forward mast island. Power was run through the ships scientific cabling from the main laboratory to the forward mast island (Old SIL radiometer loom). Special thanks to Robin Pascall of the SOC for providing the instrument.

Other meteorological measurements. Atmospheric pressure was determined using a Vaisala HMP-5 barometer unit. Cloud, swell wave and sea state statistics were computed from hourly visual observations made from the ships bridge. Daily weather predictions were determined from weather fax charts as received.

Upper air profiles. In conjunction with the UK Meteorological office (UKMO) and BAS, a radiosonde receiving station comprising of a Beukers receiver unit and a Vaisala PP-11 processor logging to a PC was installed on the JCR and daily upper air profiles of temperature, pressure and humidity were made at approximately 10:30 local time. Table 4 and figure 13 summarize the release positions for the entire ROSSA 1996 experiment. Vaisala RS-80 sonde units were used to profile for temperature pressure and humidity. 5 sonde units were faulty due to either incorrect pressure sensor readings, no carrier or no data frequency present in the signal. Some releases were also made at night when clear sky conditions were present at the time of ERS-2 ATSR satellite overpass. All data were reported to the UKMO in near real time via the ships radio officer. Thanks go to Jenny Rust (BAS) for organization and operation of the Radiosonde system and to John Shanklin (BAS) for ensuring the radiosonde system was operational.

2.4 Satellite Data

ERS-2 ATSR satellite data has been archived by RAL which will be validated using the RAL SISTeR radiometer system. Over 15 validation data sets were collected although cloud cover may reduce this number further. Special thanks are due to Chris Mutlow and his team at RAL for access to both the SISTeR radiometer and ERS-2 ATSR data. Radiosonde balloon launches were made at regular intervals throughout the cruise as described above some of which were released at ERS-2 ATSR night time overpass time for validation purposes. NOAA AVHRR HRPT data has been ordered from the Dundee satellite receiving station, the BAS ARIES receiving station and AVHRR GAC data is currently archived at the University of Boulder. These data will be intercompared and validated with the ROSSA 1996 and ERS-2 ATSR data. Specifically, the synergistic use of the ATSR instrument as a SSST calibration source for the AVHRR will be investigated.

2.5 Sea surface roughness. (In collaboration with D. Lyzenga, University of Michigan)

Sea surface roughness was determined using radar backscatter measurements made at 10.252 GHz (X band) using a continuous wave Doppler radar system. The radar was mounted on the forward mast of the JCR to view the same area as the radiometer systems and oriented to receive vertically polarized radiation at an angle of 45° . The sample frequency of this system is 512 Hz and is an experimental system which has been developed for use at sea. Configuration problems prevented data collection at the beginning of the cruise which were resolved via e-mail communication. Radar measurements were then collected and archived to dedicated PC data logger and backed up by an Iomega tape streamer at regular intervals. The large volume of data generated by this system requires that future deployments include a large data storage capacity reducing the number of backups required. These data are currently being analysed.

2.6 CO_2 measurements - (Cliff Law, PML)

Continuous measurements of atmospheric and surface water CO_2 were made by C Law of Plymouth Marine Laboratories (PML) using an autonomous analytical instrument designed at PML. The computer controlled system

consists of a series of solenoids which direct gas samples from a percolating packed bed equilibrator, a pumped air supply from the ships bridge ad two WMO traceable standards, to an infra-red transmissometer (LiCOR). The system is also equipped with a GPS system so that measurements are logged relative to time and position. Initial problems were experienced due the lack of maintenance and attention given to the system following its use on previous cruises. Initial blockage of the marine air line was cleared and a PTFE trap installed to try to prevent this in future. Water had penetrated in both marine air and equilibrator gas lines, and consequently the system was badly corroded internally. As a result the system required a complete mechanical overhaul during the first few days of the cruise, after which the system ran continuously from 49 N to 35 S. After shutdown for four days in Montevideo the system required further maintenance with replacement of an air pump and a solenoid valve, but data collection continued between 33 N and Port Stanley. Some software problems were experienced during the cruise but these had minor impact on data collection.

Generally the pCO_2 data shows variability over shelf, upwelling and frontal regions associated with elevated productivity, increased nutrient availability and enhanced mixing. Undersaturation was observed in the higher latitudes around 45 N, resulting from the relatively more rapid cooling of these waters compared to the rate of re-equilibrium with the atmosphere. Of particular note is the region of undersaturation centered on 5 N (see Figure 14) which has been measured on a previous cruise (AMT-1). This feature exhibited similar levels of undersaturation on both cruises, of approximately 20-30 matm, but was more spatially restricted than on AMT-1 to 3 N to 7.5 N. Once again this feature was associated with a salinity minimum of < 35 psu. Also apparent in Figure 14 is an area of undersaturation around 10 S, which exhibited a maximum drawdown of 20 matm. This feature was also observed during AMT-1, but was not associated with a salinity minimum. It should be noted that these are preliminary data and have not been filtered for atmospheric contamination from ships emissions whilst on station and have been temperature corrected using BSST data as opposed to SSST derived from the radiometric observations. ROSSA 1996 radiometric SSST data will be used in a collaborative study to investigate the effect of SSST calibration corrections to pCO_2 data and on the current computations for the piston velocity exchange coefficients.

3 Summary

The ROSSA 1996 experiment has generated a state of the art data set accurate enough for the detailed investigation of the sea surface skin temperature difference (ΔT) and the investigation of the transport of heat and momentum at the air sea interface. Together with the measurements made by the AMT-3 experiment, the exchange of temperature soluble gasses across the air sea interface and the relationship between the deep subsurface temperature and the skin temperature can also be investigated. Undoubtedly the advances in technology and design which have produced the SISTeR radiometer mean that ROSSA 1996 data set is unrivaled in terms of the accuracy of infra-red radiometer measurements previously made. The extent of data coverage for much of the data set is continuous across the Atlantic ocean with breaks only due to poor weather or calibration runs. The data set includes many cloud free days where several skin temperature validation pairs will be derived for both the ERS-2 ATSR and the NOAA AVHRR series of satellite radiometer. Of particular interest is the validation of the ERS-2 ATSR and the current algorithms used at the BAS AVHRR HRPT AIRES receiving station (Rothera base). The ROSSA data set will be used as a foundation for the development of both a skin and a bulk sea surface temperature retrieval algorithm in the South Atlantic for use with the AIRES data as well as a validation data base for the synergistic use of satellite radiometer systems.

The exchange of CO_2 across the air-sea interface and the implications for oceanic uptake have been studied by many authors in the past and it is vital that the behavior and cycling of CO_2 is well understood. The ROSSA-AMT-3 data set is the first data set to have explicit measurements of both the carbon flux and the precise skin temperature together made over such a large range of conditions. These data will be used to generate a set of skin temperature transfer coefficients for CO_2 for comparison with other published data. Further, the drawdown of CO_2 shown in figure 14 will also be investigated in terms of the skin temperature deviation.

The failure of the OPHIR MISTRC radiometer was a large blow to the experiment as the data derived from this instrument would have been directly compared to that obtained by the SISTeR radiometer. This would have been a direct comparison between the two distinctly different calibration methods used by each system over a broad range of conditions. As

a result, it is recommended that the OPHIR MISTRC radiometer have a through overhaul before any further deployment including replacement of all cables and external connections. However in the course of attempting to repair the MISTRC radiometer several problems with the current system were discovered the main one being the effect of water being lifted off the calibration bucket water surface and splashed over the instrument lenses. This is a serious problem when the instrument is deployed in exposed regions such as the ships bow used during ROSSA 1996. It is recommended that a protection system be constructed minimizing this effect using a series of baffles. Further modifications include a complete redesign of the calibration bucket to lower the center of gravity and allow sufficient drainage.

The lack of a continuous vertical temperature profile in the top 2 m of the water surface especially during the day is a limitation of the ROSSA 1996 data set. The diurnal variability in the upper layers of the ocean can be significant and complicate the measurement of SSST using radiometric data. Ideally in these conditions a detailed vertical profile through the air - sea interface would enable a more thorough investigation of the SSST deviation in such conditions. However this will involve the development of specific high resolution profiling temperature sensors or vertical sensor arrays.

Of particular note is the requirement to either fully protect the SOOSR instrumentation or provide some means to periodically calibrate the instrumentation while at sea. Further modifications to log the data streams via the Oceanlogger RhoPoint interface should also be undertaken reducing the number of back ups required from a data logger system often placing equipment such as laptop PC's in danger while working in exposed areas such as the foredeck or mast.

4 References

Allen, M. R., C. T. Mutlow, G. M. C. Blumberg, J. R. Christy, R. T. McNilder, and D. T. Llewellyn-Jones, Global Change Detection., *Nature, 370*, 24-25, 1994

Coppin P. A., E. F. Bradley, I. J. Barton and J. S. Godfrey, Simoultaneous observations of sea surface temperature in the western equatorial pacific ocean by bulk, radiative and satellite methods., *J. Geophys. Res, 96 (Supp)*, 3401-3409, 1991.

Donlon, C. J. and I. S. Robinson, Observations of the oceanic thermal skin in the Atlantic ocean, *Submitted to J. Geophys Res, 1996.*

Edwards, T., Browning, R., Delderfield, J., Lee, D. J., Lidiard, K. A., Milburrow, R. W., McPherson, P. H., Peskett, S. C., Toplis, G. M., Taylor, H. S., Mason, I., Mason, G., Smith, A. and Stringer, S., The Along Track Scanning Radiometer- Measurement of Sea-Surface Temperature from ERS-1, *J. of the British Interplan. Soc., 43*, 160-180. 1990

Hadley Centre for Climate Prediction and Research, Climate Data Requirements., *Meteorological Office, Braknell ,Berks*, 1994.

Hasse, L. and P. S. Liss, Gas exchange across the air-sea interface., *Tellus, 32*, 470-481, 1981.

Jessup A. T and V. Hesany, Modulation of ocean skin temperature by swell waves. *J. Geopys. Res., 101*, 6501-6511, 1996

Mutlow, C. T., Závody, A. M., Barton, I. J. and Llewellyn-Jones, D. T., Sea Surface Temperature Measurements by the Along-Track Scanning Radiometer on ERS-1 Satellite: Early Results., *J. Geophys. Res., 99*, 22575-22588, 1994

Robertson, J. E. and Watson, A. J., Thermal skin effectof the surface ocean and its' implications for CO2 uptake., *Nature, 358*, 738-740, 1992

Robinson, I. S., N. C. Wells, and H. Charnock., The Sea Surface Thermal Boundary Layer and its Relevance to the Measurement of Sea Surface Temperature by Airborne and Spaceborne Radiometers.,*Int. J. Rem. Sensing, 5*, 19-45, 1984.

Schleussel, P., Emery, W. J., Grassl, H. and Mammen, T., On the Bulk Skin Temperature Difference and its Impact on Satellite Remote Sensing of Sea Surface Temperature. *J. Geophys. Res., 95*, 13,341-13,356, 1990

Stephens, M. P., G. Samuels, D. B. Olsen and R. A. Fine, Sea-air flux of CO_2 in the north Pacific using shipboard and satellite data., *J. Geophys Res., 100,* 15571-15583, 1995.

Van Scoy, K. A., Morris, K. P., Robertson, J. E. and Watson, A. J., Thermal skin effect and the air-sea flux of carbon dioxide: A seasonal high resolution estimate., *Glob. Biogeochem. Cycles, 9*, 253-262, 1995

5 Figure captions

1. Ship track taken during ROSSA 1996 AMT-3 cruise.

2. Typical single channel signal data generated by the SISTeR radiometer. Claerly seen are the hot and clod blackbody traces, sea surface trace and the sky radiance trace. Note units are in counts.

3. ROSSA 1996 SISTeR data transects.

4. Preliminary calibrated SISTeR data for a 15 hour period collected in the South Atlantic 22 October 1996. clearly seen is a difference in signal characteristics between hour 5 and 10 associated with a large internal wave field surface slicks.

5. Individual SOOSRtransects made during ROSSA 1996.

6. Calibration curves obtained using a CASOTS black body unit before and after the TASCO THI-500 radiometer fore optics became contaminated.

7. Example SOOSR sky and sea view data plots including the period shown in figure 4.

8. Calibration curves obtained using a CASOTS balck body unit for two separate calibrationsw of the Keyence IT2-60 radiometer.

9. Daily 15 minute samples of the entire ROSSA 1996 bulk SST at 5.5 m depth.

10. UOR transects completed during AMT-3.

11. Daily 15 minute samples of wind speed for ROSSA 1996.

12. Calibrated Solarimeter and Pyrgemoeter data for a 3 day period begining 21st September 1996. Instrumrnts were located on gimball mounts at the top of the forward mast.

13. Positions of all radiosonde ascents made during ROSSA 1996.

14. Delta pCO−2 and surface salinity plotted as a function of latitude for the AMT-3 experiement. (C Law).

6 Appendices

Appendix A: Addresses of ROSSA 1996 and AMT-3 cruise participants

Jim. Aiken, UOR/optics Plymouth Marine laboratory Prospect Prospect Place, West Hoe, Plymouth, PL1 3DH UK	phone direct line (01752) 633429 switchboard (01752) 633100 fax (01752) 633101 e.mail r.barlow@pml.ac.uk
Tony Bale, Principal Scientist Plymouth Marine laboratory Prospect Prospect Place, West Hoe, Plymouth, PL1 3DH UK	phone direct line (01752) 633425 switchboard (01752) 633100 fax (01752) 633101 e.mail a.bale@pml.ac.uk
Ray Barlow, Pigments/filtration Plymouth Marine Laboratory Prospect Prospect Place, West Hoe, Plymouth, PL1 3DH UK	phone direct line (01752) 633461 switchboard (01752) 633100 fax (01752) 633101 e.mail r.barlow@pml.ac.uk
Andrew Bowie, Dissolved/dissolvable iron Department of Env. Sciences (Davy Room 106) University of Plymouth, Drakes Circus PLYMOUTH PL4 8AA	phone: (01752) 233019 at UoP fax: (01752) 233035 e-mail: abowie@plymouth.ac.uk
Craig Donlon, ROSSA Colorado Centre for Astrodynamics Research University of Colorado Boulder CO80302, USA	tel: +303 fax: +303 email: cjdn@colorado.edu
Chris Gallienne, Zooplankton Plymouth marine Laboratory Prospect Prospect Place, West Hoe, Plymouth, PL1 3DH UK	phone direct line (01752) 633414 switchboard (01752) 633100 fax (01752) 633101 e.mail c.gallienne@pml.ac.uk
Colin. Griffiths, Physical Oceanography Plymouth Marine Laboratory Prospect Prospect Place, West Hoe, Plymouth, PL1 3DH UK	phone direct line (01752) 633274 switchboard (01752) 633100 fax (01752) 633102 e-mail crg@ pml.ac.uk
Stanford Hooker, Remote sensing optics NASA/GSFC/Code 970.2 Greenbelt, MD 20771 USA	phone: 301-286-9503 fax: 301-286-1775 Net: stan@ardbeg.gsfc.nasa.gov
Ignacio Huskin, Zooplankton Universidad de Oviedo Dept. Biologia de Organismos y Sistemas Campus del Cristo E-33071 OVIEDO, Spain	phone 0034 85 104790 fax 0034 85 104777 e.mail ihuskin@sci.cpd.uniovi.es
Cliff Law, Bio gases Plymouth Marine Laboratory Prospect Prospect Place, West Hoe, Plymouth, PL1 3DH UK	phone direct line (01752) 633425 switchboard (01752) 633100 fax (01752) 633101 e.mail c.law@pml.ac.uk

Appendix A: continued

Emilio Maranon, Productivity Southampton Oceanography Centre European Way Southampton, SO14 3ZH	phone (01703) 596110 fax (01703) 593059 e.mail: em@soton.ac.uk
Yoshihisa Mino, NASDA Optics/pigments Institute for Hydrospheric-Atmospheric Sciences, Nagoya University Chikusa-ku Nagoya 464-01, JAPAN	e.mail: kuro@ihas.nagoya-u.ac.jp
Beatriz Mourino, Productivity Universidad de Vigo Departmento de recursos Naturais e Medio Ambiente Campus Lagoas-Marcosende E-36200 Vigo Spain	
Tim Nightingale, ROSSA Space Science Dept Rutherford Appleton Laboratory Chilton, Didcot Oxfordshire OX11 0QX	phone: +44 1235 445688 fax: +44 1235 445848 email: t.j.nightingale@rl.ac.uk
Koji Suzuki, NASDA Optics/pigments Institute for Hydrospheric-Atmospheric Sciences, Nagoya University Chikusa-ku Nagoya 464-01, JAPAN	phone: +81-52-789-3490 fax: +81-52-789-3436 e-mail: kojis@ihas.nagoya-u.ac.jp
Yasunori Terrayama, NASDA/ ROSSA Saga University 1 Honjo Saga 840 JAPAN	e-mail: terra@ is.saga-u.ac.jp
Mike Zubkov, Nanoplankton/ production University of Southampton Biomedical Sciences Building Bassett Crescent East Southampton, SO16 7PX	phone (01703) 594387 fax (01703) 594269 e.mail m.v.zubkov@soton.ac.uk

Appendix B CTD-rosette water bottle log

station	266	267	268	269	270
CTD 1	none	none	7	7	7
production		due to	20	20	20
& chem		gantry	30	30	30
(m)		failure	40	40	40
			50	50	50
			60	60	60
			100	80	80
			150	100	100
			200	150	150
				200	200
CTD 2	2	none	2	7	2
pigments	6	due to	7	20	7
& zoop	10	gantry	20	30	20
(m)	20	failure	30	40	30
	30		40	50	40
	50		50	60	50
	70		60	80	60
			100	100	80
			150	150	100
				200	150

NB for 269, cast 1 was pigments and cast 2 productivity

station	271	272	273	274	276
CTD 1	80m	7	7	7	7
production	150m	20	20	20	20
& chem	200m	40	30	30	30
(m)		60	40	40	40
		80	50	50	50
		100	60	60	60
		110	80	80	80
		120	100	100	100
		150	150	150	150
		200	200	200	200
CTD 2	aborted:	2	2	2	2
pigments		7	7	7	7
& zoop		20	20	20	20
(m)		40	50	30	40
		60	80	40	45
		80	100	50	50
		100	102	60	60
		110	110	80	80
		120	120	100	100
		150	150	150	150

station	277	278	279	280	281
CTD 1	7	7	7	7	7
production	20	20	20	20	30
& chem	30	40	40	40	50
(m)	40	50	60	50	70
	50	60	70	65	90
	60	70	80	75	100
	80	80	90	85	110
	100	100	100	100	120
	150	150	120	120	140
	200	200	200	200	200
CTD 2	2	2	2	2	2
pigments	7	7	7	7	7
& zoop	20	20	40	20	50
(m)	30	30	60	40	80
	40	40	70	60	90
	45	60	78	80	100
	60	74	90	90	110
	80	90	100	100	120
	100	100	120	120	130
	150	150	150	150	150

station	282	283	284	285	286
CTD 1	7	7	7	7	7
production	25	30	25	20	40
& chem	50	60	50	40	70
(m)	75	80	75	60	80
	100	100	100	80	95
	120	120	110	90	110
	130	140	125	100	120
	140	160	140	120	140
	160	180	160	160	160
	200	200	200	200	200
CTD 2	2	2	2	2	2
pigments	7	7	7	7	7
& zoop	50	50	30	20	20
(m)	75	80	60	40	40
	100	100	90	60	60
	120	120	110	80	80
	130	140	125	100	95
	140	160	140	120	110
	160	180	160	130	120
	200	200	200	150	150

station	287	288	289	290	297
CTD 1	7	7	7	7	2
production	50	20	10	20	7
& chem	80	40	20	30	20
(m)	90	50	30	40	30
	100	60	40	50	40
	110	70	50	60	50
	120	80	60	80	60
	150	100	80	100	100
	200	150	150	150	150
		200	200	200	200
CTD 2	2	2	2	2	2
pigments	7	7	7	7	7
& zoop	30	20	10	20	20
(m)	60	40	20	30	30
	70	50	30	40	40
	80	60	40	50	50
	90	80	50	60	59
	100	100	60	80	80
	120	120	80	100	100
	150	150	150	150	150

station	298	299			
CTD 1	7	2			
production	20	7			
& chem	40	20			
(m)	60	30			
	70	40			
	80	50			
	100	60			
	120				
	150				
	200				
CTD 2	2	only one			
pigments	7	cast :-			
& zoop	20	shallow			
(m)	40	water.			
	50	All			
	70	material			
	80	from one			
	100	bottle			
	120				
	150				

Appendix C List of station positions

Day	Lat itude	Longitude	
266	N 49° 40.49	W 05° 41.42	
267	N 48° 25.10	W 12° 30.20	(no CTDs -gantry failure)
268	N 47° 21.96	W 18° 12.46	
269	N 42° 43.04	W 19° 48.81	
270	N 38° 10.13	W 20° 00.78	
271	N 34° 01.98	W 21° 15.45	(limited cast due to bottle misfires)
272	N 29° 29.58	W 21° 48.46	
273	N 24° 40.64	W 21° 24.09	
274	N 20° 05.14	W 20° 37.74	(gantry failure: extra 4hrs on station)
275	no hydrographic station due to EEZ restrictions		
276	N 12° 45.58	W 20° 32.68	
277	N 09° 03.14	W 22° 16.55	
278	N 05° 10.20	W 24° 00.98	
279	N 01° 17.37	W 25° 46.90	
280	S 02° 23.36	W 27° 27.25	
281	S 06° 29.02	W 29° 16.23	
282	S 10° 46.78	W 31° 14.46	
283	S 14° 53.44	W 33° 07.30	
284	S 18° 51.91	W 35° 02.76	
285	S 22° 55.87	W 36° 57.27	
286	S 26° 36.91	W 39° 36.05	
287	S 29° 51.04	W 42° 54.70	
288	S 32° 48.01	W 46° 96.98	
289	S 35° 42.73	W 49° 34.01	
290	S 37° 48.40	W 52° 11.63	
	292-296 In Montevideo		
297	S43° 34.71	W55° 00.36	
298	S48° 00.12	W55° 52.84	
299	S51° 55.88	W57° 53.64	

Appendix D Scientific bridge log (up to Montevideo only) All times are in GMT

Date	SDY	Latitude	Longitude	Time	Activity
22/09/96	266	N 49° 40.1'	W 5° 40.2'	0800	Stopped on station #1 (trial)
				0822	CTD deployed (water depth 86m)
				0826	CTD at 70m
				0836	Optical rig deployed
				0852	CTD recovered
				0853	Optical rig recovered
				1000	Plankton net deployed
				1007	Plankton net recovered
				1020	Station complete
				1030	UOR deployed
				1035	UOR deployed to 400m
				1500	UOR recovered
23/09/96	267	N 48° 24.7'	W 12° 30.0'	0930	Stopped on station #2
				0945	Optical rig deployed
				0947	CTD deployed - oil leak from hydraulic hose on midship gantry
				0950	CTD recovered
				1020	Plankton net deployed 200m (1st cast)
				1037	Optical rig at surface
				1039	Optical rig recovered
				1043	Plankton net recovered
				1048	Plankton net redeployed 20m (2nd cast)
				1050	Plankton net recovered
				1053	Optical rig redeployed to 50m
				1055	Surface drift net deployed
				1101	Optical rig recovered
				1108	Floating buoy unit deployed
				1117	Plankton net recovered
				1130	Floating buoy unit recovered
				1200	Station complete
				1205	UOR deployed
				1315	UOR recovered on-board to change rig
				1335	UOR fully deployed to 430m
		N 48°11.0'	W 13°46.6'	1807	XBT launched
				1937	UOR recovered onto deck
24/09/96	268	N 47°21.9'	W 18°12.7'	1030	Stopped on station #3
				1039	Optical rig and CTD deployed
				1043	CTD at 200m
				1046	Plankton net deployed 200m (1st cast)
				1102	Optical rig recovered
				1104	Plankton net recovered
				1108	CTD recovered
				1109	Plankton net redeployed 100m (2nd cast)
				1112	Plankton net recovered
				1115	Drift net deployed
				1130	Drift net recovered
				1145	CTD redeployed to 200m
				1208	CTD recovered
				1226	Station complete
				1235	UOR deployed
				1238	XBT aborted - problems with software
				1436	UOR recovered
				2325	XBT launched
25/09/96	269	N 42°54.0'	W 19°59.5'	1030	Stopped on station #4

				1040	CTD, optical rig, plankton net deployed (1st cast)
				1045	CTD at 200m
				1053	Optical rig recovered
				1054	Plankton net recovered
				1058	Plankton net redeployed (2nd cast)
				1100	Plankton net recovered
				1106	Drift net deployed
				1110	CTD recovered
				1112	Optical rig deployed
				1125	Drift net recovered
				1135	CTD deployed; optical rid recovered
				1138	Drift buoy deployed
				1155	CTD recovered
				1159	Drift buoy recovered
				1212	Station complete
				1220	XBT launched
				1455	Thermometer in water from Port side
26/09/96	270	N 38°10.13	W 20o0.78'	0005	XBT launched
				1125	Stopped on station #5
				1132	CTD deployed
				1133	Plankton net deployed (1st cast)
				1145	Drift buoy deployed
				1149	Plankton net recovered
				1154	Plankton net deployed (2nd cast)
				1106	CTD recovered
				1110	Plankton net recovered; drift buoy recovered
				1122	Drift net deployed
				1140	CTD deployed
				1145	Drift net recovered
				1146	Optical rig recovered
				1203	CTD recovered
				1207	Station complete
				1211	XBT launched
				1220	UOR fully deployed to 370m
				1926	UOR recovered and secured
				2300	XBT launched
27/09/96	271	N 34°01.6'	W 21°15.3'	0700	XBT launched
				1125	Stopped on station #6
				1127	Optical rig, plankton net deployed (1st cast)
				1130	CTD deployed to 200m
				1145	Plankton net recovered
				1150	Plankton net redeployed (2nd cast)
				1152	Plankton net recovered
				1154	Plankton net redeployed (3rd cast)
				1205	CTD recovered
				1210	Drifting buoy deployed; CTD redeployed; plankton net recovered
				1215	Drift net deployed
				1223	CTD recovered
				1224	Drifting buoy recovered
				1230	Optical rig redeployed - aborted
				1236	Drift net recovered
				1240	CTD redeployed; optical rig redeployed
				1250	Optical rig recovered
				1253	CTD recovered
				1303	CTD deployed to 80m
				1315	CTD recovered
				1320	Station complete

				1330	UOR deployed to 370m
				1330	XBT launched
				1837	UOR recovered
28/09/96	272			0115	XBT launched
				0726	XBT launched
		N 29°29.7'	W 21°48.4'	1125	Stopped on station #7
				1130	Plankton net (1st cast), optical rig deployed
				1134	CTD deployed to 200m
				1145	Plankton net recovered
				1150	Plankton net redeployed (2nd cast)
				1200	CTD recovered
				1212	Plankton net recovered
				1214	Optical rig recovered
				1216	Drift net deployed
				1223	Drifting buoy deployed
				1241	Drifting buoy recovered
				1245	Drift net recovered
				1252	CTD recovered
				1300	Station complete
				1304	UOR deployed to 375m
				1725	UOR recovered
				2130	XBT launched
29/09/96	273			0950	XBT launched
		N 24°40.6	W 21°24.0	1125	Stopped on station #8
				1127	Plankton net deployed (1st cast)
				1130	CTD (200m), optical rig deployed
				1145	Plankton net recovered
				1147	Plankton net redeployed (2nd cast)
				1150	Plankton net recovered
				1157	Plankton net redeployed (3rd cast)
				1209	Plankton net recovered
				1212	Drift net deployed
				1215	Optical rig recovered
				1220	Drifting buoy deployed
				1245	Drift net recovered; drifting buoy (NASA) deployed
				1255	Rocket buoy deployed
				1300	CTD recovered
				1305	NASA buoy recovered
				1310	Station complete
				1317	UOR deployed to 375m
				1605	XBT launched
				1655	UOR recovered
				2100	XBT launched
30/09/96	274			0100	XBT launched
				0500	XBT launched
				0900	XBT launched
		N 20°04.1'	W 20°33.7'	1055	Stopped on station #9
				1100	Plankton net (1st cast), optical rig deployed
				1105	Oil leak on midship gantry; CTD aborted
				1120	Plankton net recovered
				1121	Plankton net redeployed (2nd cast)
				1125	Plankton net recovered
				1126	Plankton net redeployed (3rd cast)
				1140	Optical rig recovered
				1142	Drifting buoy deployed
				1145	Drift net deployed
				1205	Drift net, drifting buoy recovered

				1215	Drift buoys (NASA) deployed
				1240	NASA buoys recovered
				1245	NASA buoys redeployed
				1320	NASA buoys recovered
				1345	Free Fall reference redeployed
				1405	Free Fall rocket redeployed
				1432	Free Fall reference recovered
				1435	Free Fall rocket recovered
				1440	Midship gantry deployment test - all OK
				1450	CTD deployed
				1521	CTD recovered
				1550	CTD redeployed
				1615	CTD recovered
				1620	Station complete
				1638	XBT launched
01/10/96	275			0120	XBT launched
				0450	XBT launched
				0930	XBT launched
				1540	XBT launched
02/10/96	276			0115	XBT launched
				0930	XBT launched
		N 12°45.6'	W 20°32.7'	1055	Stopped on station #10
				1100	Optical rig deployed
				1104	Plankton net deployed 200m (1st cast)
				1108	CTD deployed 200m
				1122	Plankton net recovered
				1125	Plankton net redeployed 20m (2nd cast)
				1128	Plankton net recovered
				1130	CTD recovered; plankton net redeployed 200m (3rd cast)
				1137	Optical rig recovered
				1145	Plankton net recovered; drifting buoy launched
				1152	Drift net deployed
				1200	Drifting buoy recovered
				1201	NASA buoy deployed; CTD redeployed
				1206	Rocket buoy deployed
				1215	Drift net recovered
				1224	CTD recovered
				1225	NASA buoys recovered
				1230	Station complete
				1240	UOR deployed to 380m
				2030	UOR recovered
03/10/96	277			0120	XBT launched
		N 9°39'	W 21°59'	0700	UOR deployed to 380m
				0920	UOR recovered
				0940	XBT launched
		N 9°03.0'	W 22°16.5'	1055	Stopped on station #11
				1100	Optical rig; plankton net (1st cast) deployed
				1102	CTD deployed
				1116	Plankton net recovered
				1122	Plankton net redeployed (20m, 2nd cast)
				1123	Plankton net recovered
				1125	Plankton net redeployed (200m, 3rd cast); CTD recovered
				1135	Optical rig recovered
				1138	Optical rig redeployed
				1145	Optical rig recovered
				1149	Plankton net recovered

				1151	Drifting buoy deployed; CTD deployed
				1153	Drift net deployed
				1210	Drifting buoy recovered
				1212	CTD recovered; NASA freefall buoy deployed
				1225	Drift net recovered
				1230	NASA buoy recovered
				1235	Station complete; UOR deployed
				1710	XBT launched
				2025	UOR recovered
				2130	XBT launched
04/10/96	278			0100	XBT launched
				0450	XBT launched
				0800	UOR deployed
				0835	XBT launched
				1050	UOR recovered
		N 5°10.5'	W 24°00.6'	1055	Stopped on station #12
				1100	Plankton net deployed (1st cast); optical rig deployed
				1105	CTD deployed
				1125	Plankton net recovered
				1128	Plankton net redeployed (20m, 2nd cast); CTD recovered
				1130	Plankton net recovered
				1131	Plankton net redeployed (200m, 3rd cast)
				1134	Light meter recovered
				1139	Light meter deployed
				1146	Plankton net recovered
				1150	Drift net deployed
				1152	CTD deployed; light meter recovered, buoy deployed
				1210	CTD recovered; Plankton net recovered
				1215	Drifting buoy recovered
				1216	Freefall buoys deployed
				1225	Freefall buoys recovered
				1230	Station complete; UOR deployed to 360m
				1455	UOR recovered
				2215	XBT launched
05/10/96	279			0515	XBT launched
				0925	XBT launched
		N 1°17.3'	W 25°46.9'	1055	Stopped on station #13
				1058	Optical rig deployed
				1105	Plankton net (1st cast) deployed; CTD deployed
				1114	Plankton net recovered
				1116	Plankton net redeployed (20m, 2nd cast)
				1118	Plankton net recovered
				1122	Plankton net redeployed (200m, 3rd cast)
				1125	CTD recovered
				1130	Optical rig recovered
				1132	Optical rig deployed
				1134	Optical rig recovered
				1136	Drifting buoy deployed; plankton net recovered
				1140	Drift net deployed
				1148	CTD deployed
				1155	Drifting buoy recovered
				1210	Drift net recovered; CTD recovered
				1215	Station complete
				1223	UOR deployed
				1225	XBT launched

				2013	XBT launched
		0°00.0'	W 26°21.3'	2016	Vessel crosses equator
				2230	XBT launched
06/10/96	280			0040	XBT launched
				0320	XBT launched
				0525	XBT launched
				0707	UOR recovered
				0726	XBT launched
		S 2°23.4'	W 27°27.2'	1055	Stopped on station #14
				1100	Plankton net deployed(1st cast); optical rig deployed
				1103	CTD deployed
				1113	Plankton net recovered
				1116	Plankton net redeployed (20m, 2nd cast)
				1120	Plankton net recovered
				1122	Plankton net redeployed (200m, 3rd cast); optical rig recovered; CTD recovered
				1128	Drifting buoy deployed
				1136	Plankton net recovered
				1140	Drift net deployed
				1145	Drifting buoy recovered
				1150	Freefall buoys deployed; CTD deployed
				1210	Freefall buoys recovered; CTD recovered
				1212	Drift net recovered
				1220	Station complete
				1223	UOR deployed to 360m
				1225	XBT launched
				1625	XBT launched
				1650	UOR recovered
				2130	XBT launched
07/10/96	281			0200	XBT launched
				0845	XBT launched
		S 6°29'	W 29°16'	1055	Stopped on station #15
				1100	Optical rig, plankton net (1st cast), CTD deployed
				1113	Plankton net recovered
				1116	Plankton net deployed (20m, 2nd cast)
				1120	Plankton net recovered
				1123	Drifting buoy deployed
				1126	Optical rig recovered; CTD recovered
				1134	Optical rig deployed; plankton net recovered
				1137	Drift net deployed
				1146	Optical meter recovered
				1150	Drifting buoy recovered
				1200	Freefall buoys deployed; CTD deployed
				1211	Drift net recovered
				1214	CTD recovered
				1216	Freefall buoys recovered
				1220	Station complete
				1225	UOR deployed; XBT launched
				1810	UOR recovered
08/10/96	282			0330	XBT launched
				0848	XBT launched
		S 10°46.8'	W 31°14.4'	1155	Stopped on station #16
				1200	Plankton net deployed (200m, 1st cast)
				1201	CTD, optical rig deployed
				1215	Plankton net recovered
				1216	Drifting buoy deployed; Plankton net redeployed (20m, 2nd cast)

				1220	Plankton net recovered; optical rig recovered
				1221	Plankton net redeployed (200m, 3rd cast)
				1240	Plankton net recovered; freefall buoys deployed
				1245	Drift net deployed
				1250	CTD deployed
				1305	Freefall buoys recovered
				1310	Drift net recovered; CTD recovered
				1315	Station complete
				1325	XBT launched
09/10/96	283			0205	XBT launched
				0800	XBT launched
		S 14°53'	W 38°06.9'	1215	Stopped on station #17
				1219	Plankton net deployed (200m, 1st cast)
				1228	CTD, optical rig deployed
				1230	Drifting buoy deployed
				1233	Plankton net recovered
				1235	Plankton net redeployed (20m, 2nd cast)
				1237	Plankton net recovered
				1240	Plankton net redeployed (3rd cast)
				1245	CTD recovered
				1249	Optical rig recovered
				1255	Plankton net recovered
				1256	Drift net deployed
				1300	Freefall buoys deployed
				1313	CTD deployed
				1327	Drift net recovered
				1330	Freefall buoys recovered
				1335	CTD recovered - bottles did not fire
				1340	CTD redeployed
				1404	CTD recovered
				1412	Station complete; UOR deployed to 360m
				1415	XBT launched
				1852	UOR recovered
				2040	XBT launched
10/10/96	284			0205	XBT launched
		S 18°51.8'	W 35°02.7'	1155	Stopped on station #18
				1200	Plankton net (1st cast); CTD deployed
				1201	Optical rig deployed
				1205	Drifting buoy deployed
				1218	Plankton net recovered
				1220	Plankton net redeployed (20m, 2nd cast)
				1222	Plankton net recovered
				1225	Plankton net redeployed (200m, 3rd cast)
				1230	Drifting buoy, CTD recovered
				1245	Freefall buoy deployed
				1246	Plankton net recovered
				1247	Drift net deployed
				1255	CTD deployed
				1310	Freefall buoys recovered
				1319	CTD, plankton nets recovered
				1321	Station complete
				2033	XBT launched
11/10/96	285			0210	XBT launched
				0945	XBT launched
		S 22°55.9'	W 36°57.2'	1155	Stopped on station #19
				1200	Plankton net deployed (1st cast)
				1202	CTD, drifting buoy deployed
				1205	CTD aborted: no fluorescence signal

				1212	Plankton net recovered
				1215	Plankton net redeployed (20m, 2nd cast)
				1216	Plankton net recovered
				1217	Plankton net redeployed (200m, 3rd cast)
				1222	CTD deployed; drifting buoy recovered
				1228	Freefall buoys deployed
				1233	Plankton net recovered
				1235	Drift net deployed
				1245	CTD recovered
				1307	Plankton net recovered
				1310	Freefall buoys recovered
				1315	CTD redeployed
				1340	CTD recovered
				1345	Station complete
				1347	UOR deployed
				1610	UOR recovered
		S 23°20.9'	W 37°10.4'	1613	Stopped on station #20 (optics only)
				1615	Reference deployed
				1618	Rocket deployed
				1647	Reference recovered
				1652	Rocket recovered; station complete
				1700	UOR deployed
12/10/96	286	S 26°36.9'	W 39°36.0'	1155	Stopped on station #21
				1200	Optical rig, CTD, plankton net (1st cast) deployed
				1209	Drifting buoy deployed
				1213	Plankton net recovered
				1215	Plankton net redeployed (2nd cast)
				1217	Plankton net recovered
				1220	Plankton net redeployed (3rd cast)
				1225	Optical rig, CTD recovered
				1235	Plankton net recovered; freefall buoys deployed
				1236	Drift net deployed
				1255	CTD deployed
				1305	Drift net recovered
				1315	CTD, freefall buoys recovered
				1320	Station complete
				1335	XBT launched
		S 27°00.1'	W 40°00.8'	1600	Stopped on station #22 (optics only)
				1611	Optical rig deployed
				1632	Optical rig recovered
				1642	Reference deployed
				1645	Rocket deployed
				1656	Reference, rocket recovered
				1700	Station complete
				1722	XBT launched
13/10/96	287			0135	XBT launched
		S 29°51'	W 42°54'	1200	Stopped on station #23
				1201	Plankton net deployed (1st cast)
				1202	CTD deployed
				1212	Plankton net recovered
				1215	Plankton net redeployed (2nd cast)
				1217	Plankton net recovered
				1218	Plankton net redeployed (3rd cast)
				1227	CTD recovered
				1232	Plankton net recovered
				1235	Drift net deployed
				1255	CTD redeployed
				1302	Drift net recovered
				1315	CTD recovered

				1326	Station complete
				1328	UOR deployed
				1910	UOR recovered
				2020	XBT launched
14/10/96	288			0055	XBT launched
				0840	XBT launched
		S 32°48'	W 46°07'	1200	Stopped on station #24
				1202	Plankton net (1st cast), CTD, optical rig deployed
				1215	Plankton net recovered
				1220	Plankton net redeployed (2nd cast)
				1222	Plankton net recovered
				1224	Plankton net redeployed (3rd cast)
				1228	CTD recovered
				1238	Optical rig recovered
				1240	Plankton net recovered
				1243	Drift net deployed
				1258	CTD redeployed
				1315	Drift net recovered
				1318	CTD recovered
				1320	Station complete
				1326	UOR deployed
				1335	XBT launched
				1900	UOR recovered
				1905	XBT launched
15/10/96	289			0305	XBT launched
		S 35°42.7'	W 49°24.2'	1230	Stopped on station #25
				1234	Plankton net (1st cast), optical rig deployed
				1242	Drifting buoy deployed
				1245	CTD deployed
				1250	Plankton net recovered
				1251	Plankton net redeployed (2nd cast)
				1254	Plankton net recovered
				1255	Plankton net redeployed (3rd cast)
				1310	Drifting buoy, CTD, optical rig, plankton net recovered
				1315	Drift net deployed
				1326	Freefall buoys deployed
				1338	CTD redeployed
				1345	Drift net recovered
				1350	Freefall buoys recovered
				1400	CTD recovered
				1405	Station complete
				1410	XBT launched; UOR deployed
				1705	UOR recovered
		S 36°05.4'	W 50°03.4'	1710	Stopped on station #26 (optics only)
				1712	Reference and rocket deployed
				1732	Reference and rocket recovered
				1743	Optical rig redeployed
				1812	Optical rig recovered
				1815	UOR deployed to 360m
				2010	UOR recovered
				2011	XBT launched
				2105	UOR redeployed
16/10/96	290			0300	XBT launched
				1145	UOR recovered
		S 37°48'	W 52°11.6'	1150	Stopped on station #27
				1155	Plankton net deployed (1st cast)
				1157	CTD deployed to 200m

				1200	Optical rig deployed
				1205	Drifting buoy deployed
				1208	Plankton net recovered
				1211	Plankton net redeployed (2nd cast)
				1213	Plankton net recovered
				1215	Plankton net deployed
				1225	CTD recovered
				1227	Optical rig recovered
				1230	Plankton net recovered
				1232	Drift net deployed; drifting buoy recovered
				1240	Freefall buoys deployed
				1254	CTD redeployed
				1306	Plankton net, freefall buoys recovered
				1319	CTD recovered
				1330	Station complete
22/10/96	296	S 38°41.2'	W 55°00.3'	1640	XBT launched
		S 40°20.6'	W 54°59.4'	2340	XBT launched
23/10/96	297	S 42°46'	W 55°59'	0930	XBT launched
		S 43°34'	W 55°01.5'	1255	Stopped on station #28
				1300	Plankton net deployed (200m, 1st cast)
				1305	Light meter deployed
				1310	CTD deployed
				1312	Drifting buoy deployed
				1320	Plankton net recovered
				1323	Plankton net redeployed (20m, 2nd cast)
				1325	Plankton net recovered
				1326	Plankton net redeployed (200m, 3rd cast)
				1330	Light meter recovered
				1335	Drifting buoy recovered
				1342	CTD recovered
				1343	Plankton net recovered
				1346	Drift net deployed
				1350	Freefall buoys deployed
				1408	CTD redeployed
				1415	Freefall buoys recovered
				1417	Plankton net recovered
				1420	CTD cable jammed and jumped out of traction winch - unable to recover
				1520	CTD wire repair complete; continue deployment
				1526	Resume hauling CTD slowly and firing bottles
				1530	CTD wire strand caught
				1535	Resume hauling
				1546	CTD recovered
				1548	Station complete
		S 43°33.8'	W 55°00.3'	1554	UOR deployed
		S 43°33.8'	W 55°00.3'	1555	XBT launched
		S 43°49.3'	W 55°04.4'	1720	XBT launched
		S 44°00.8'	W 55°02.0'	1815	XBT launched
		S 44°05.8'	W 55°00.6'	1845	XBT launched
		S 44°15'	W 55°00'	1930	XBT launched
		S 44°24'	W 55°00'	2015	XBT launched
		S 44°36.3'	W 54°59.3'	2115	XBT launched
		S 44°36'	W 54°59'	2120	UOR recovered
		S 44°59.9'	W 54°58.1'	2305	XBT launched
24/10/96	298	S 45°13.1'	W 54°58.3'	0005	XBT launched
		S 45°26.4'	W 55°00.2'	0105	XBT launched
		S 45°50.3'	W 55°04.9'	0305	XBT launched

		S 46°17.7'	W 55°07.8'	0450	XBT launched
		S 46°47.4'	W 55°20.3'	0705	XBT launched
		S 47°46.8'	W 55°47.0'	1145	XBT launched
		S 48°00.7'	W 55°52.8'	1255	Stopped on station #29
				1258	Plankton net deployed (200m, 1st cast)
				1301	Optical rig deployed
				1302	CTD deployed
				1310	Drifting buoy deployed
				1315	Plankton net recovered
				1317	Plankton net deployed (2nd cast)
				1320	Plankton net recovered
				1330	Optical rig recovered
				1332	CTD recovered
				1337	Drifting buoy recovered
				1340	Drift net deployed
				1342	Freefall buoys deployed
				1400	CTD redeployed
				1415	Freefall buoys, drift net recovered
				1425	CTD recovered
				1430	Station complete
		S 48°00.8'	W 54°52.3'	1435	UOR deployed, XBT launched
		S 48°50.8'	W 56°16.5'	1915	UOR recovered
25/10/96	299	S 50°27.7'	W 57°02.9'	0320	XBT launched
		S 51°55.8'	W 57°53.6'	1100	Stopped on station #30
				1105	Plankton net deployed (1st cast)
				1106	CTD deployed
				1107	Plankton net recovered
				1110	Plankton net redeployed (2nd cast)
				1115	Plankton net recovered
				1118	Optical rig, drift net deployed
				1135	Optical rig recovered
				1136	Drift net recovered
				1145	CTD recovered; station complete

APPENDIX E: The following tables summarise the Radiosonde releases, SOOSR and SISTeR data collected during ROSSA 1996.

Filename	SDay	Time	Latitude	Longitude
22091.fli	266	10:30	49°00' 00	-005° 35' 00
23091.fli	267	10:35	48°24' 00	-012° 30' 00
24091.fli	268	10:40	47° 18' 00	-018° 12' 00
25091.fli	269	11:10	42° 54' 00	-020° 00' 00
26093.fli	270	15:20	36° 52' 09	-020° 06' 31
27091.fli	271	11:20	34° 08' 24	-021° 13' 79
28091.fli	272	10:45	29° 34' 68	-021° 48' 12
29091.fli	273	10:50	24° 44' 85	-021° 24' 97
30091.fli	274	10:55	20° 04' 14	-020° 33' 70
01101.fli	275	11:23	16° 43' 55	-020° 24' 62
02101.fli	276	12:48	12° 46' 00	-020° 32' 16
03101.fli	278	11:10	09° 02' 28	-022° 16' 51
04101.fli	279	11:15	05° 10' 35	-024° 00' 93
05101.fli	280	11:00	01° 17' 45	-025° 46' 91
06101.fli	281	10:55	-2° 23' 53	-027° 27' 45
07101.fli	282	11:00	-6° 28' 98	-029° 27' 45
09101.fli	284	11:10	-15° 07' 91	-032° 52' 71
10101.fli	285	11:10	-18° 45' 82	-035° 00' 09
11101.fli	286	10:05	-22° 37' 56	-036° 48' 98
12101.fli	287	09:14	-26° 11' 85	-039° 11' 90
13101.fli	288	11:20	-29° 46' 57	-042° 50' 03
15101.fli	289	01:46	-34° 23' 05	-047° 48' 22
23101.fli	297	02:33	-40° 59' 48	-055° 00' 47
23102.fli	297	17:47	-43° 51' 91	-055° 04' 67

Table 3. Radiosonde ascents made during ROSSA 1996 September - October 1996.

Filename	Start day, time,Latitude & Longitude				Stop day, time, Latitude & Longitude				Comments
21099601.tas	266	02:58	49.98761°	-003.953758°	266	08:30	49.67890°	-005.692109°	Clock_wrong_10s_tasco4.dld
21099602.tas	266	13:37	49.50886°	-006.585515°	266	19:09	49.19004°	-008.262480°	Tasco4.dld_10s
22099201.tas	266	13:37	49.50886°	-006.585515°	267	00:44	48.87919°	-009.938138°	Tasco4.dld_Data_merged_with21099202.tas
23099201.tas	267	06:20	48.85844°	-011.57698°	267	07:23	48.52643°	-011.87952°	Tasco4.dld
23099602.tas	267	07:25	48.52434°	-011.88926°	267	10:02	48.41560°	-012.50089°	Tasco4.dld
23099604.tas	267	10:04	48.41606°	-012.50122°	267	18:32	48.12481°	-014.09384°	Tasco5.dld_20s_samples
24099601.tas	269	11:41	42.90359°	-019.99188°	269	22:12	40.91995°	-020.02055°	
26099601.tas	269	22:12	40.91995°	-020.02055°	270	11:02	38.23145°	-020.00563°	Clock_1_hour_slow
26099602.tas	270	11:05	38.22121°	-020.00577°	270	22:09	36.54061°	-020.50457°	Clock_1_hour_slow
27099601.tas	270	11:05	38.22121°	-020.00577°	271	10:11	34.23990°	-021.20289°	Data_merged_with_26099602.tas_Clock_1_Hour_slow
27099602.tas	271	10:13	34.23385°	-021.20543°	271	21:03	32.59572°	-021.45913°	Clock_1_hour_slow
28099601.tas	271	21:06	32.58347°	-021.46058°	272	10:30	29.65128°	-021.79257°	Clock_1_hour_slow
28099602.tas	272	10:31	29.64772°	-021.79308°	272	21:20	27.85427°	-021.98914°	
29099601.tas	272	21:23	27.84288°	-021.99038°	273	11:14	24.69165°	-021.40668°	Clock_1_hour_slow
29099602.tas	273	11:17	24.68158°	-021.40472°	273	21:05	23.11309°	-021.11109°	
30099601.tas	273	21:08	23.10125°	-021.10871°	274	10:12	20.17384°	-020.57714°	
30099602.tas	274	10:15	20.16535°	-020.57622°	274	21:15	19.28478°	-020.41596°	
01109601.tas	274	21:17	19.27877°	-020.41610°	275	10:42	16.84978°	-020.40905°	
01109602.tas	275	10:45	16.84099°	-020.40914°	275	22:19	14.79390°	-020.40477°	
02109601.tas	275	22:22	14.78501°	-020.40417°	276	10:59	12.76050°	-020.54345°	
02109602.tas	276	11:01	12.76082°	-020.54290°	277	01:25	10.64114°	-021.54621°	
03109601.tas	277	01:28	10.63199°	-021.55088°	277	15:00	8.667257°	-022.45448°	
03109602.tas	277	15:04	8.655745°	-022.45925°	277	21:39	7.517585°	-022.92030°	
04109601.tas	277	21:55	7.465383°	-022.94053°	278	14:31	4.855253°	-024.16504°	
04109602.tas	277	21:55	7.465383°	-022.94053°	278	21:49	3.565466°	-024.74987°	2_files_together
05109602.tas	279	10:10	.1399582°	-025.73768°	280	01:01	.7819294°	-026.8702°	no_data_rain
06109601.tas	280	01:04	-.791358°	-026.69171°	280	14:34	-2.747962°	-027.62196°	
06109602.tas	280	14:36	2.750868°	-027.62323°	280	22:41	-4.188426°	-028.25129°	All_OK
07109601.tas	280	22:44	-4.196433°	-028.25488°	281	14:15	-6.807650°	-029.43122°	Lenses_cleaned
07109602.tas	281	14:18	-6.816659°	-029.43570°	281	22:49	-8.335868°	-30.12811°	
08109601.tas	281	22:52	-8.347832°	-030.13326°	282	15:11	-11.12097°	-031.40161°	
08109602.tas	282	15:14	-11.12860°	-031.40518°	283	00:38	-12.88516°	-032.21001°	
09109601.tas	283	00:41	-12.89412°	-032.21458°	283	13:43	-14.88647°	-033.12111°	
09109602.tas	283	13:46	-14.88614°	-033.12123°	284	00:57	-16.86408°	-034.04258°	
10109601.tas	284	01:00	-16.87321°	-034.04754°	284	17:00	-19.52132°	-035.32661°	
10109602.tas	284	17:03	-19.52606°	-035.32888°	285	02:05	-21.15715°	-036.12458°	
11109601.tas	285	02:08	-21.16626°	-036.12905°	285	16:22	-23.34732°	-037.17500°	

11109602.tas	285	16:26	-23.34701°	-037.17608°	286	02:19	-25.09934°	-038.09378°	
12109601.tas	286	02:21	-25.10349°	-038.09739°	286	15:59	-27.00250°	-040.01315°	
12109601.tas	287	06:02	-28.92417°	-041.97880°	287	22:38	-31.13466°	-044.29669°	RAIN_ALL_DAY_LOST_NIGHT_DATA_WRAPAROUND
12109601.tas	286	02:21	-25.10349°	-038.09739°	286	15:59	-27.00250°	-040.01315°	
13109601.tas	287	06:02	-28.9241°7	-041.97880°	287	22:38	-31.13466°	-044.29669°	RAIN_ALL_DAY_LOST_NIGHT_DATA_WRAPAROUND
14109601.tas	287	22:39	-31.13466°	-044.29699°	288	13:33	-32.80232°	-046.13219°	RAIN_IN_MORNING
14109602.tas	288	13:36	-32.81009°	-046.13966°	288	23:48	-34.11971°	-047.54582°	CLEAR_SKY_IN_EVENING
15109601.tas	288	23:51	-34.12712°	-047.55362°	289	13:32	-35.71312°	-049.59732°	JDAY_NUMBER_IS-_1
16109601.tas	290	02:12	-37.02344°	-051.14894°	290	11:54	-37.80668°	-052.19380°	OK_BEFORE_MONTE_HEAVY_SEAS
16109602.tas	290	11:57	-37.80724°	-052.19356°	290	21:45	-36.57173°	-053.60442°	BANGING_INTO_HEAVY_SEAS
17109610.tas	291	00:20	-36.61600°	-054.17110 °	291	16:58	-34.90393°	-056.22514°	IN_MONTE_AT_ANCHOR_FROM_10.00
22109601.tas	295	21:17	-34.90390°	-056.22514°	296	12:33	-37.72173°	-055.03121°	FROM_MONTE_HARBOUR_OUT
22109602.tas	296	12:35	-37.72949°	-055.03039°	296	23:51	-40.32446°	-054.98874°	LOTS_OF_SLICKS_STRUCTURE_CLEAR_SKY
23109601.tas	296	23:54	-40.40131°	-054.99427°	297	12:19	-43.45421°	-055.00069°	ATSR/2_OVERPASS_0248
23109602.tas	297	12:22	-43.46617°	-055.00086°	297	22:48	-44.95527°	-054.96994°	EXCELLENT_DAY_WARM_CORE_RINGS_ETC
24109601.tas	297	22:50	-44.96280°	-054.96914°	298	13:22	-48.00407°	-055.87643°	NIGHT_TIME_OVER_LARGE_FRONTAL_EDDY_SYSTEMS
25109601.tas	298	23:31	-49.63634°	-056.66400°	299	12:28	-61.94336°	-058.19851°	

Table 4. SOOSR transects completed during ROSSA 1996 September - October 1996.

Filename	Start day, time Latitude & Longitude				Stop day, time Latitude Longitude				Comments
22099601.arc	266	14:01:59	49.48678°	-006.70651°	266	14:18:29	49.47291°	-006.782428°	Bad_ROSSA_01.EXE
25099601.arc	269	15:27:27	42.28092°	-019.996°	269	17:01:29	41.96655°	-020.0012°	Bad_except_1st_10_minutes
25099602.arc	269	17:10:01	41.93662°	-020.003°	270	10:02:09	38.43997°	-020.00309°	Bad
27099601.arc	271	13:42:59	33.99517°	-021.28403°	272	17:11:18	28.72367°	-021.89554°	OK_Cloud
28099601.arc	272	17:49:41	28.60866°	-021.90833°	274	01:50:18	22.04665°	-020.92401°	OK_Clear_1st_6_hours
30099601.arc	274	02:01:17	21.94806°	-020.90155°	274	05:21:16	21.23424°	-020.775726°	OK_Cloud
30099602.arc	274	05:22:52	17.81269°	-020.41866°	275	09:51:09	17.00239°	-020.40903°	OK_Mostly_clear
01109601.arc	275	09:59:45	16.97802°	-020.40891°	275	10:00:28	16.97505°	-020.40906 °	Half_cycle_only
01109602.arc	275	10:09:45	16.94706 °	-020.40913°	276	16:26:06	12.16504°	-020.83968°	OK_Increased_noise
02109601.arc	276	17:04:38	12.06329°	-020.88276°	277	19:47:40	7.840012°	-022.79202°	OK_Bagged_overnight
03109601.arc	277	21:33:35	7.586839°	-022.91237°	278	16:51:58	4.446052°	-024.34930 °	OK_Mostly_clear_Door_trials
05109601.arc	278	10:06:12	5.286366°	-023.94993°	278	21:53:51	3.553919°	-024.75545°	OK_Light_cloud
05109602.arc	278	22:06:20	3.515354°	-024.77369°	279	15:56:46	0.7391555°	-026.03453°	OK_Light_cloud_clear
06109601.arc	280	16:07:37	-03.1264°	-027.73584°	281	11:45:45	-06.47932°	-029.27031°	OK_Light_cloud_clear
07109601.arc	281	12:04:40	-06.4774°	-029.26961°	282	01:11:50	-08.76472°	-030.32813°	Partly_clear__6_hours_Bagged_nighht
08109601.arc	282	01:16:44	-08.7820°	-030.33553°	282	07:54:56	-10.03534°	-030.88553°	Instrument_bagged_and_idl
08109602.arc	282	07:55:16	-10.0353°	-030.88553°	282	12:04:19	-10.77891°	-031.24280°	OK_Mostly_clear
10109601.arc	284	13:21:01	-18.8544°	-035.04966°	285	12:53:57	-22.91847 °	-036.95842°	OK_Partly_clear_New_scan_mirror
11109601.arc	285	13:34:04	-22.9080°	-036.96296°	286	14:15:30	-26.75317°	-039.73614°	OK_Partly_clear_Door_closed_2_hours
12109601.arc	286	14:26:47	-26.7822°	-039.76886°	287	10:51:34	-29.69625°	-042.75370°	OK_Partly_clear_cloudy_door_closed
15109601.arc	289	09:23:26	-35.3156°	-048.96629°	290	10:05:19	-37.95943°	-052.02258°	OK_Mainly_clear_1st_12_hours
16109601.arc	290	12:02:38	-37.8074°	-052.19313°	290	13:14:32	-37.81303 °	-052.18829°	JCR_turned_into_heavy_seas_at_end
16109602.arc	290	21:51:41	-36.5530°	-053.62651°	291	09:50:01	-35.01811°	-056.02557°	OK_Clear_1st_2_hours_Rain_at_end
20109601.arc	294	19:42:39	-34.9043°	-056.22545°	295	11:32:05	-34.90439°	-056.22545°	Montevideo_harbour_Closed_overnight
22109601.arc	296	10:55:12	-37.3422°	-055.09951°	296	23:52:36	-40.39565°	-054.99397°	OK_Clear
23109601.arc	297	00:03:57	-40.4413°	-054.99747°	297	22:58:55	-44.99475°	-054.96927 °	Clear_1st_21_hours_ATSR-2_overpass

Table 5. SISTeR transects completed during ROSSA 1996 September - October 1996.

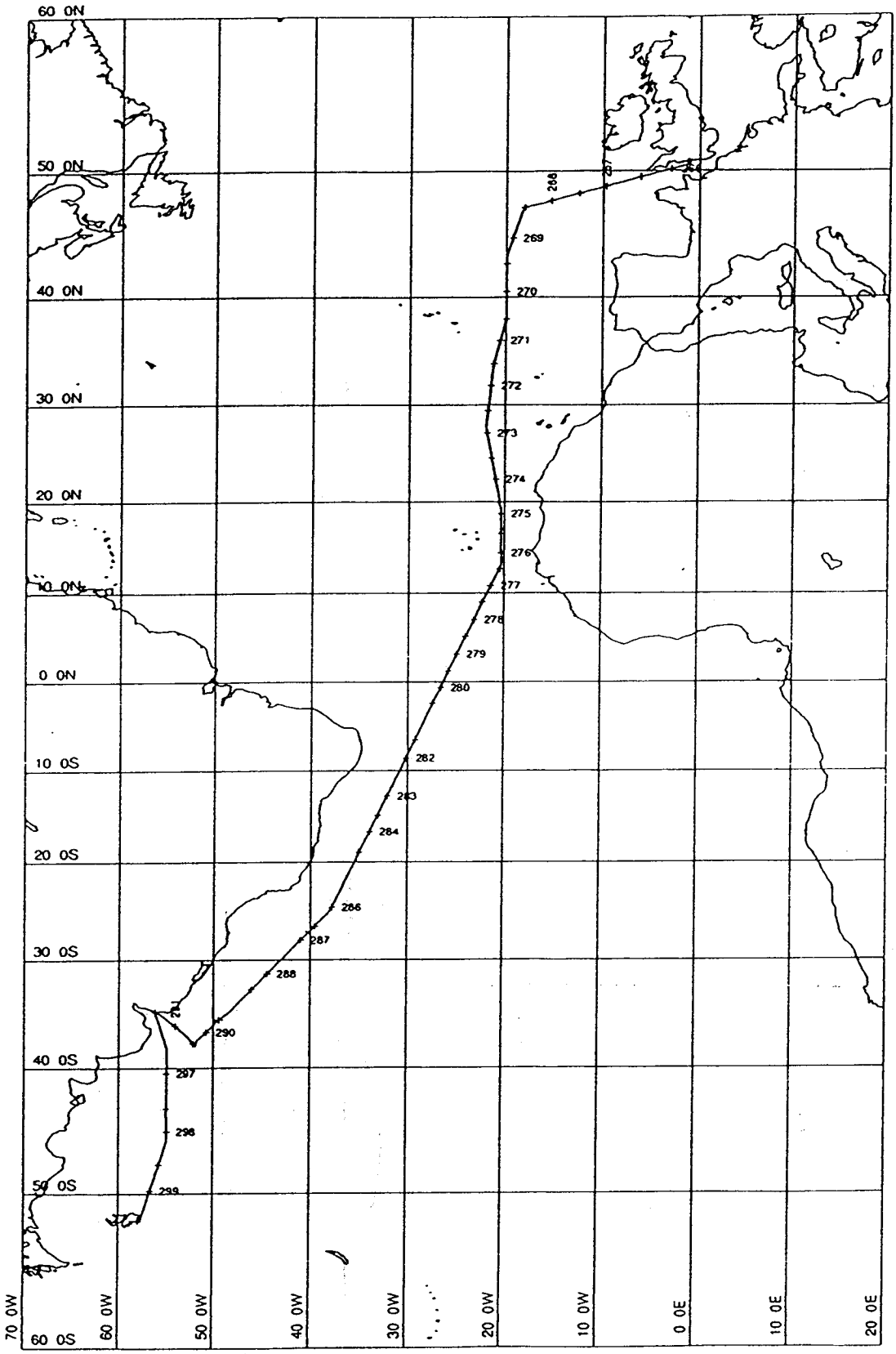

Figure 1 - Ship's track during AMT3 Cruise

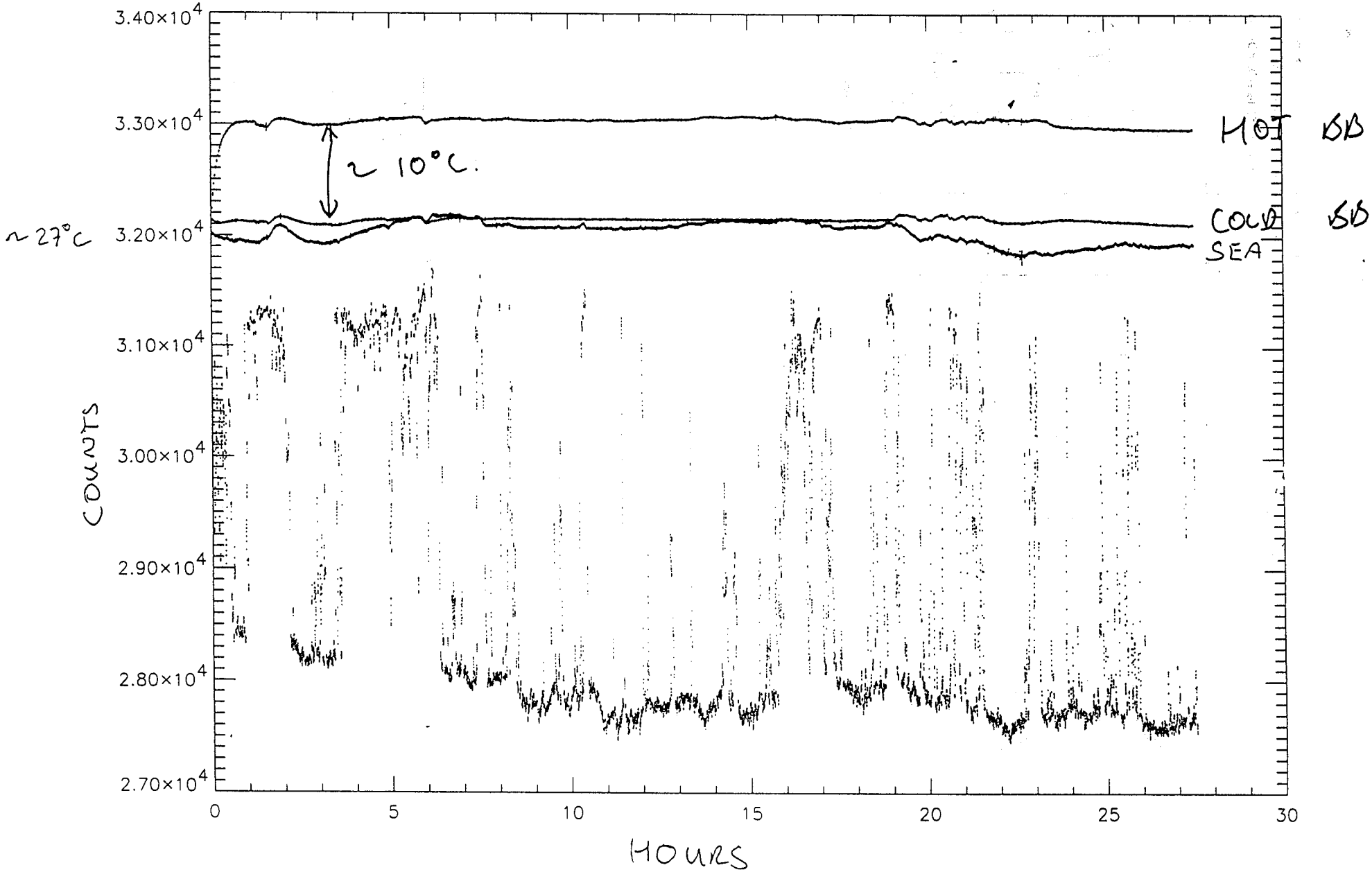
3.40×10^4
3.30×10^4
3.20×10^4
3.10×10^4
3.00×10^4
2.90×10^4
2.80×10^4
2.70×10^4
~27°C
~ 10°C.
HOT BB
COLD BB
SEA
COUNTS
0
5
10
15
20
25
30
HOURS

Figure 2

ROSSA 1996: SISTeR transects
RRS James Clark Ross September – October 1996

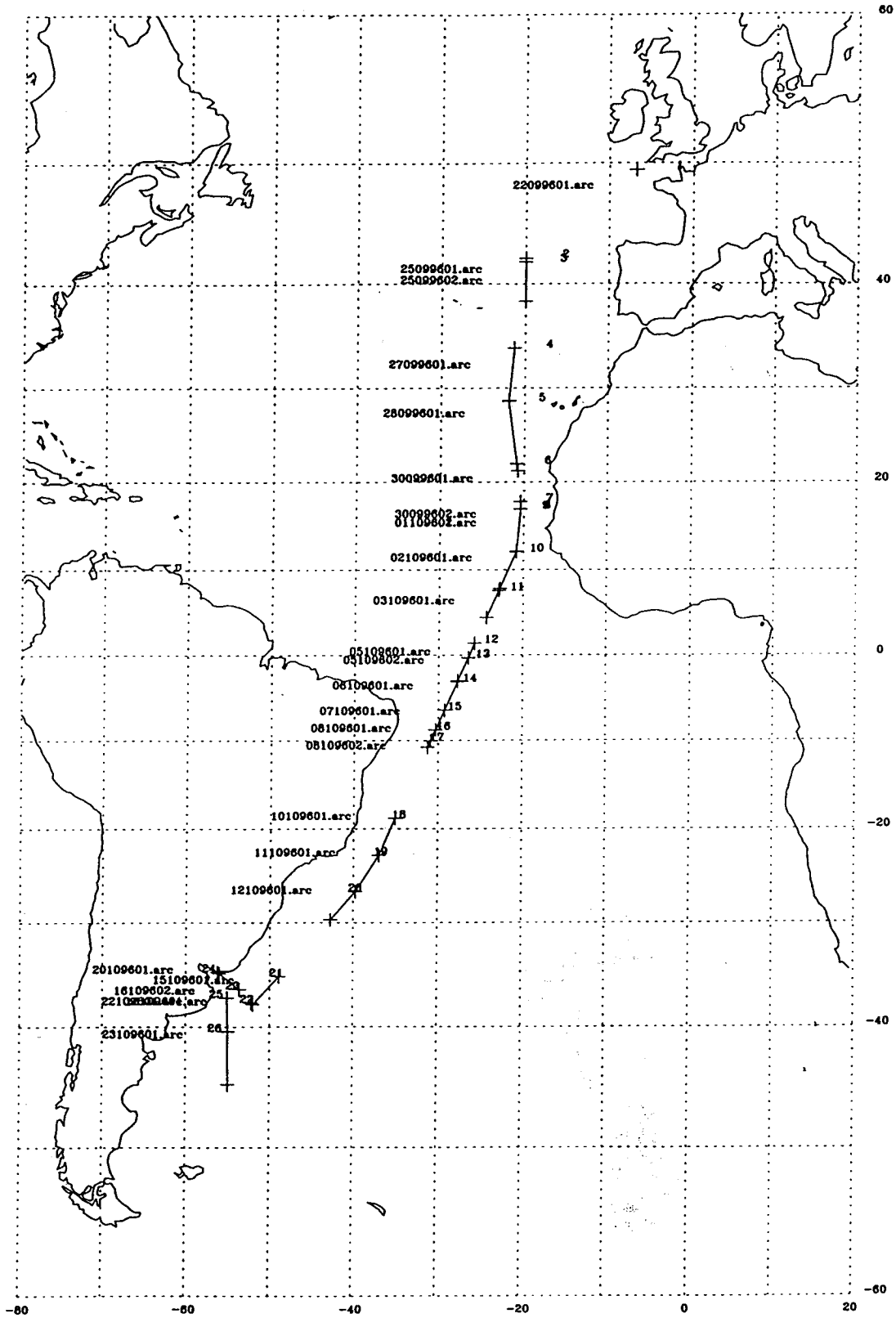

Figure 3

C J Donlon: RRS James Clark Ross, ROSSA September – October 1996.

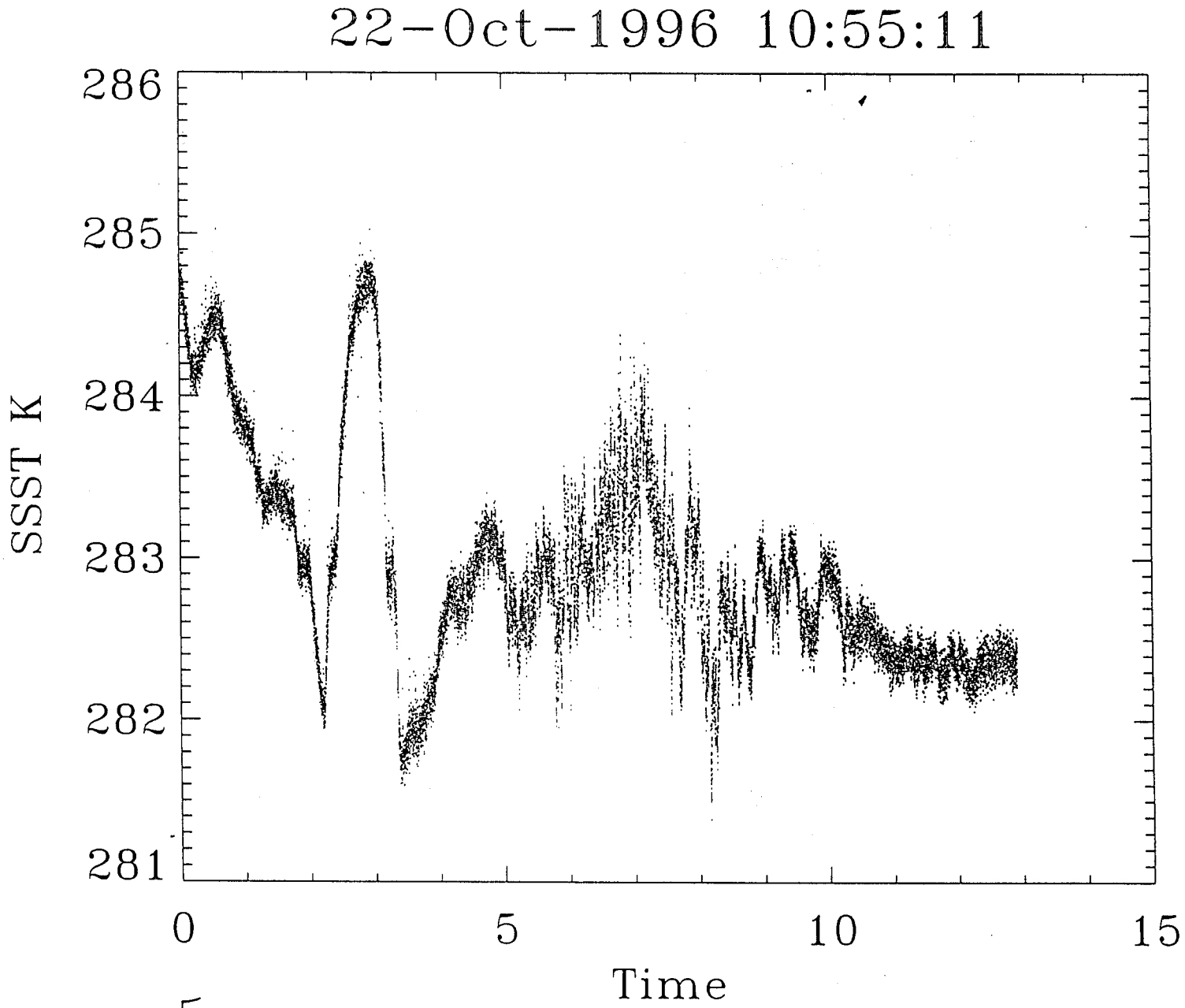

Figure 4

ROSSA 1996: SOOSR transects
RRS James Clark Ross September – October 1996

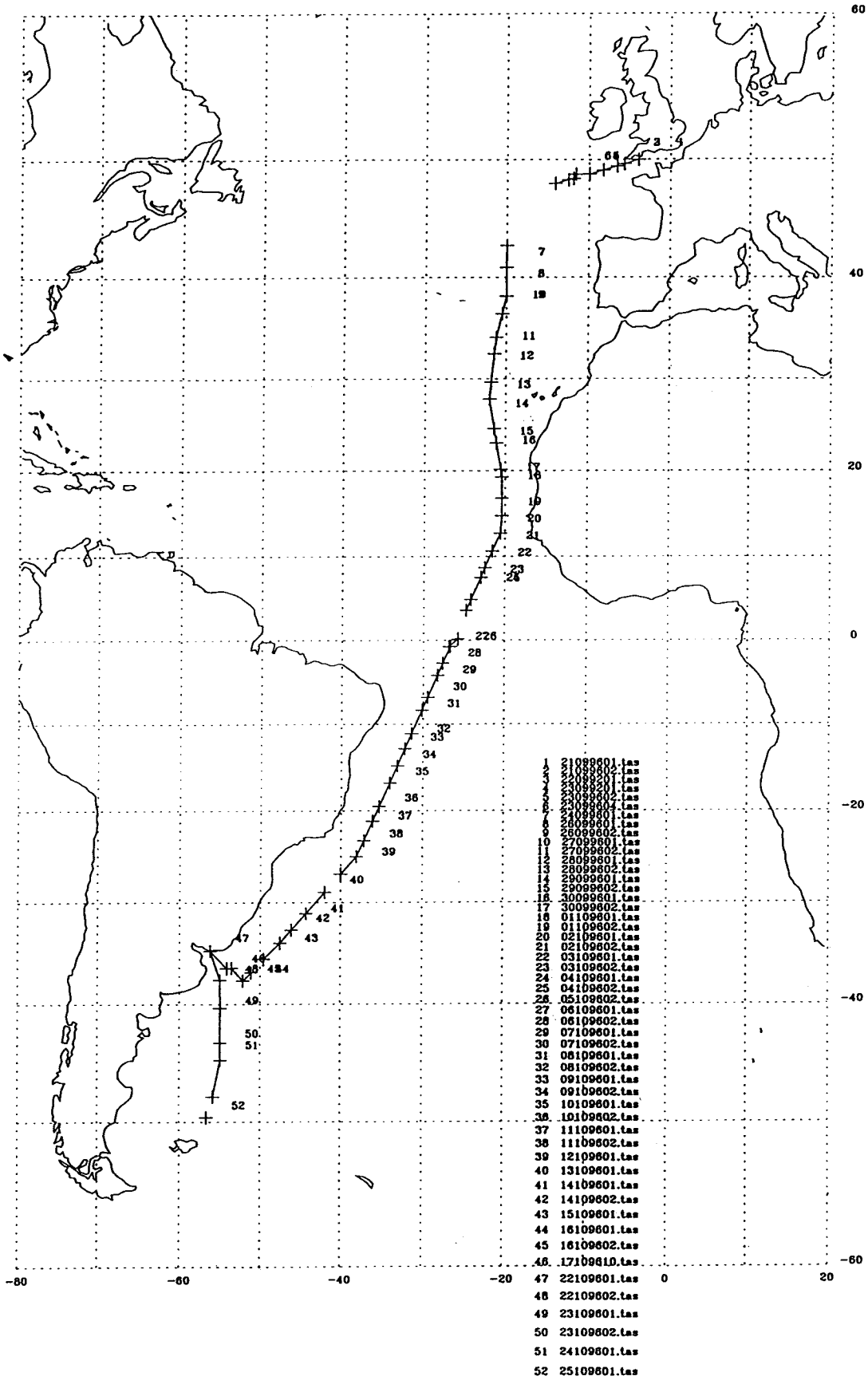

C J Donlon: RRS James Clark Ross, ROSSA September – October 1996.

Figure 5

Figure 6. TASCO THI-500 calibrations. ROSSA 1996

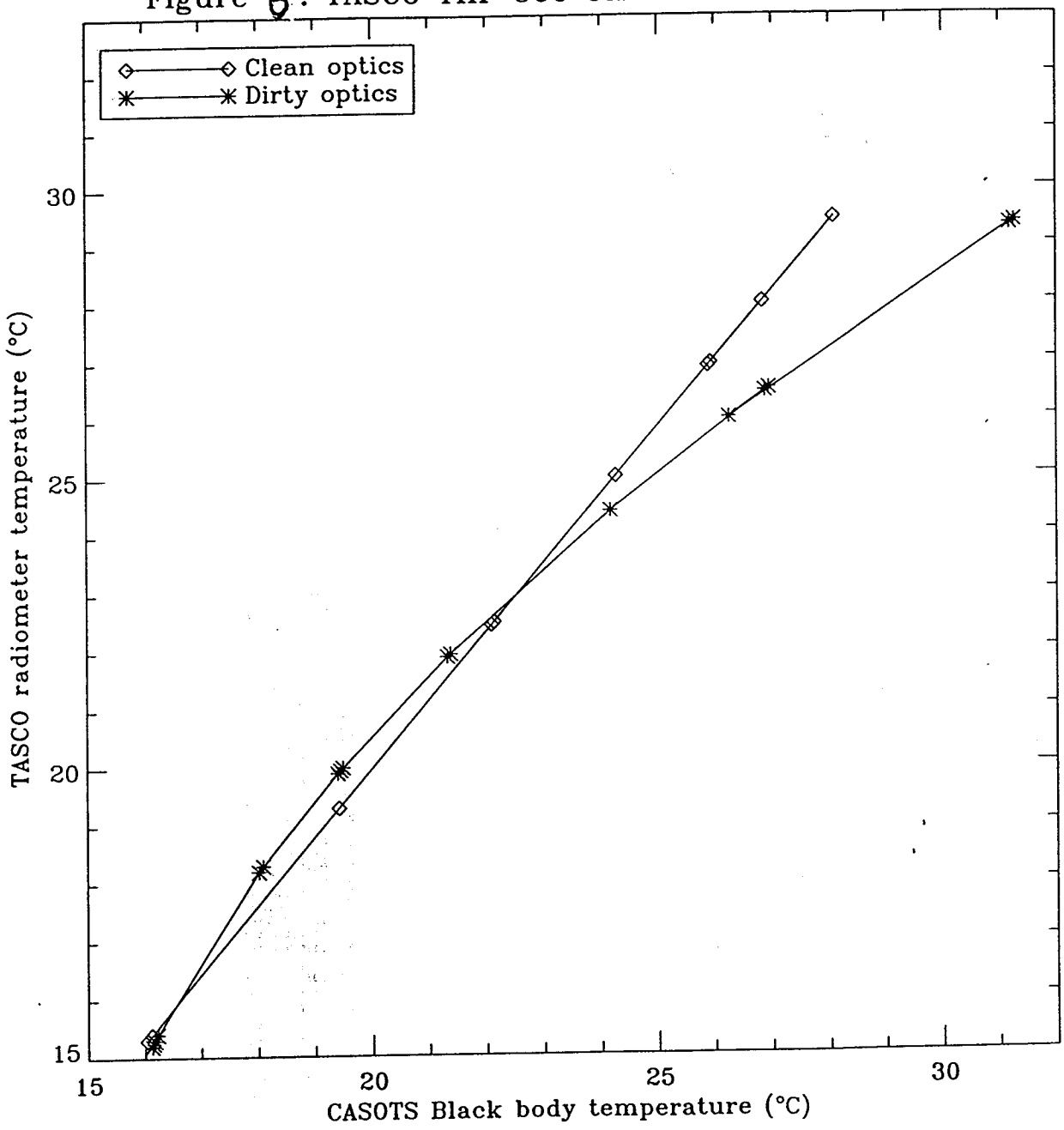

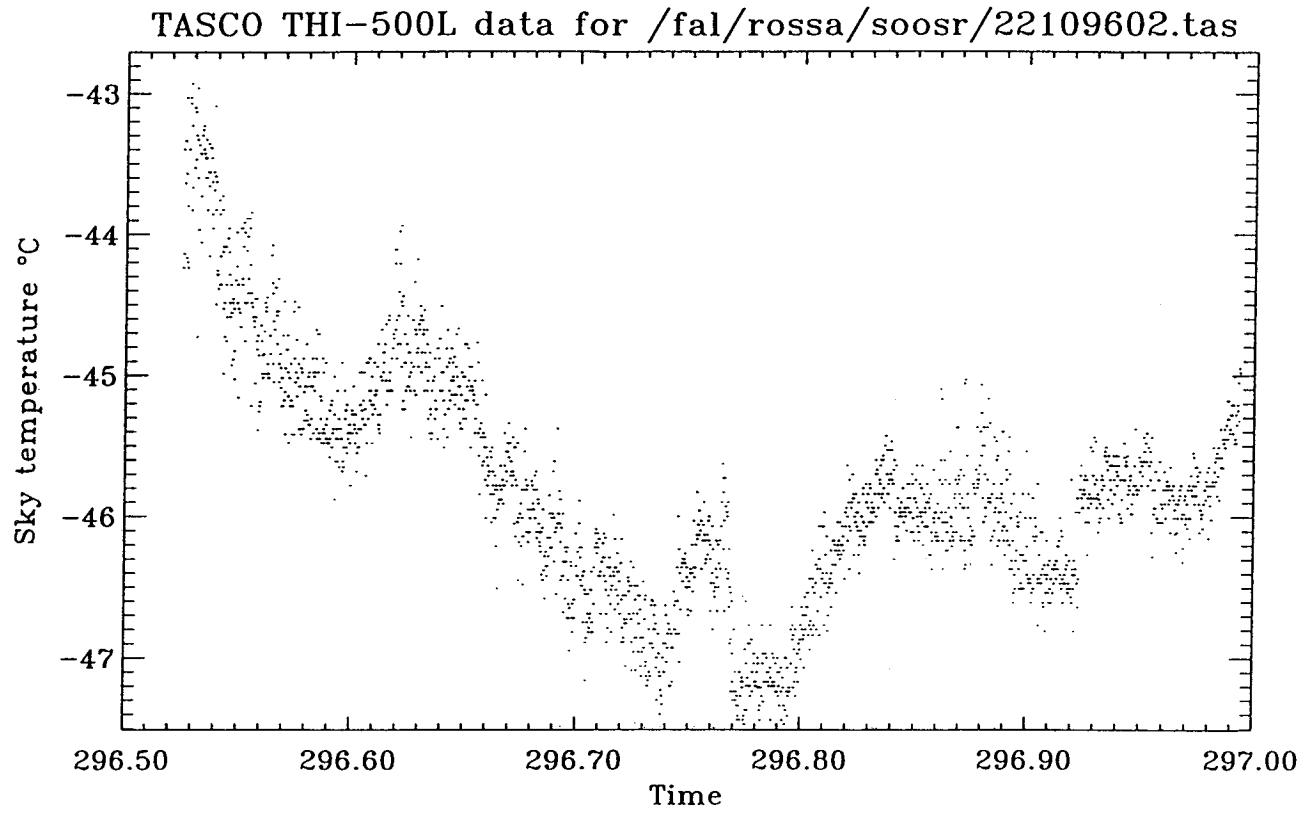
TASCO THI-500L data for /fal/rossa/soosr/22109602.tas
Sky temperature °C
-43
-44
-45
-46
-47
296.50
296.60
296.70
296.80
296.90
297.00
Time

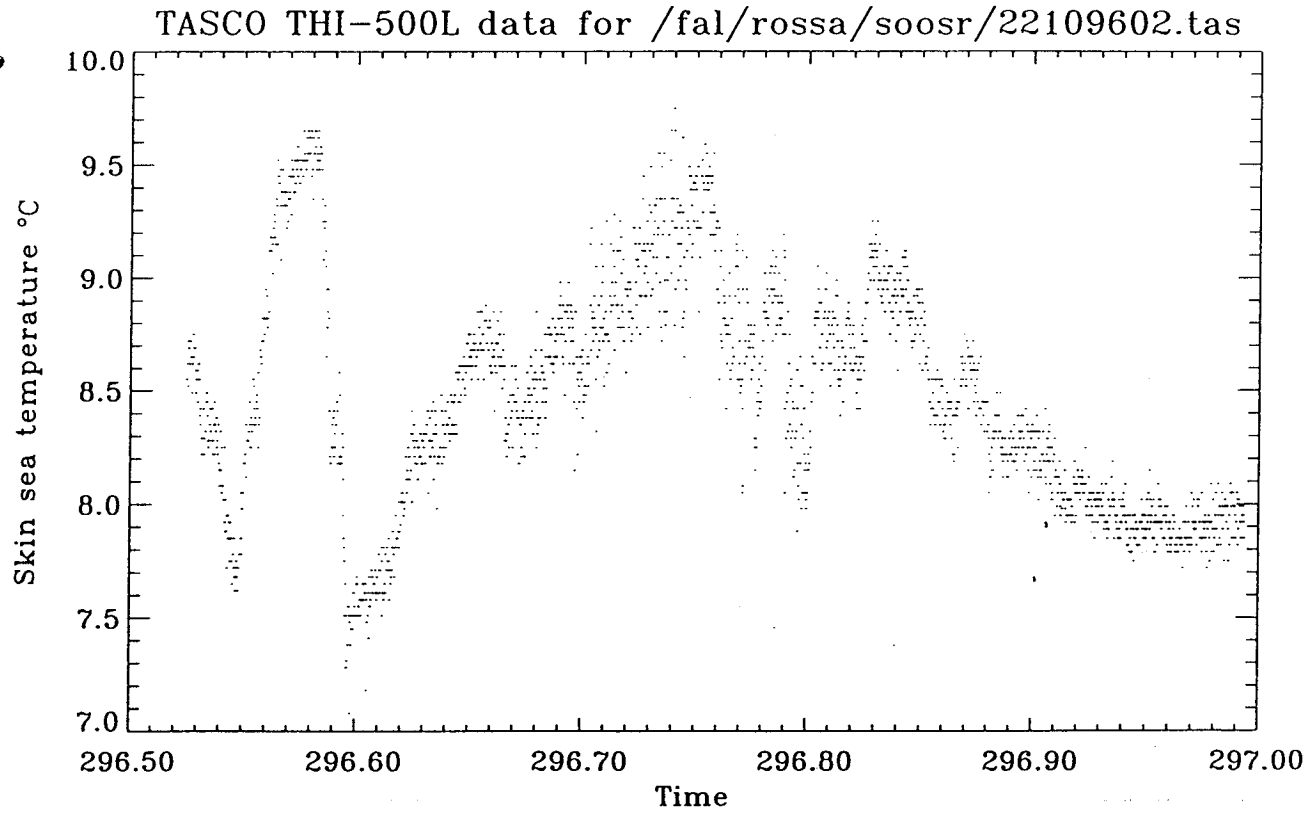
TASCO THI-500L data for /fal/rossa/soosr/22109602.tas
Skin sea temperature °C
10.0
9.5
9.0
8.5
8.0
7.5
7.0
296.50
296.60
296.70
296.80
296.90
297.00
Time

Figure 7

Figure 8 Keyence IT2-60 calibrations. ROSSA 1996

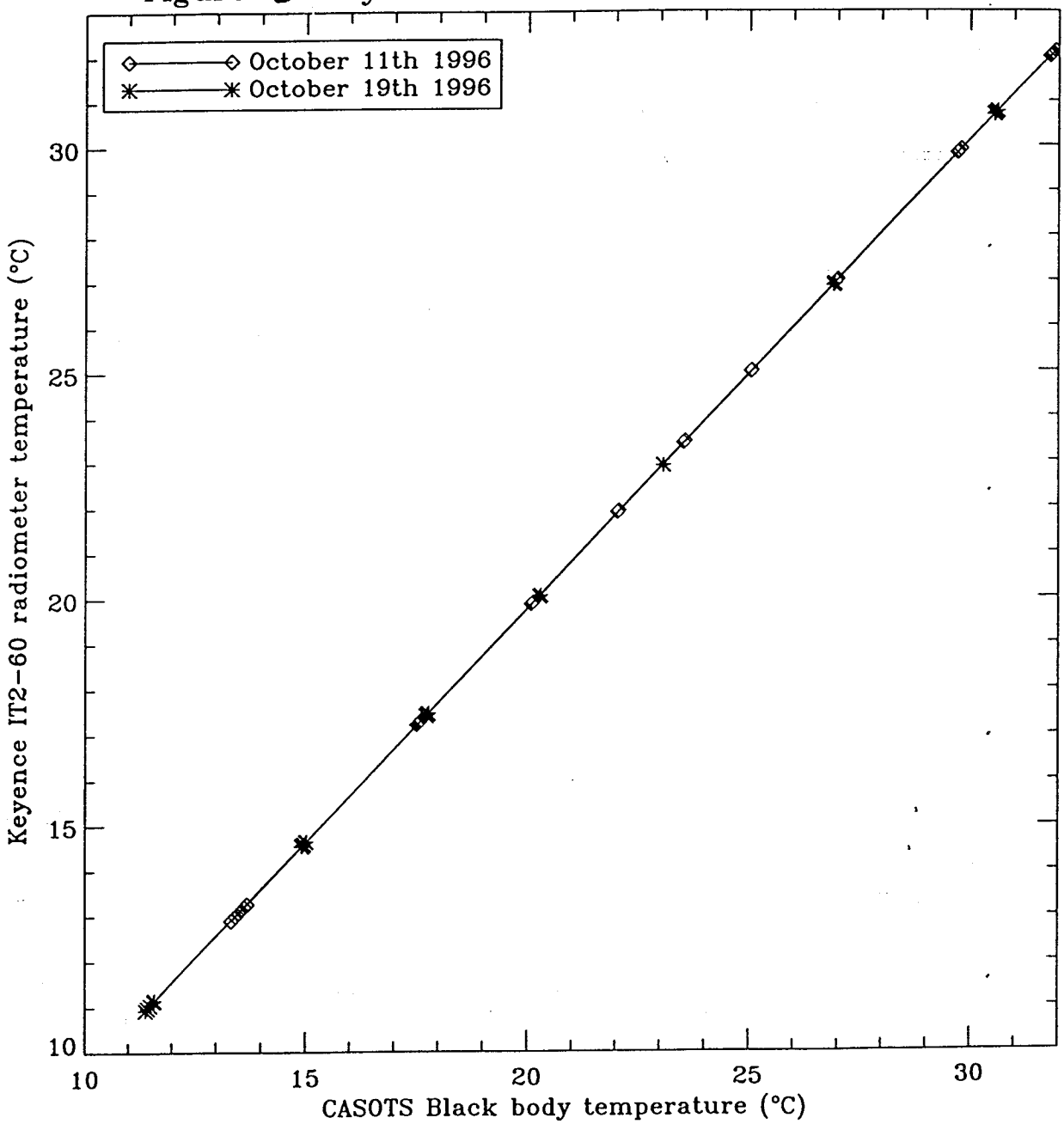

Figure 9 Range of BSST encountered during ROSSA 1996

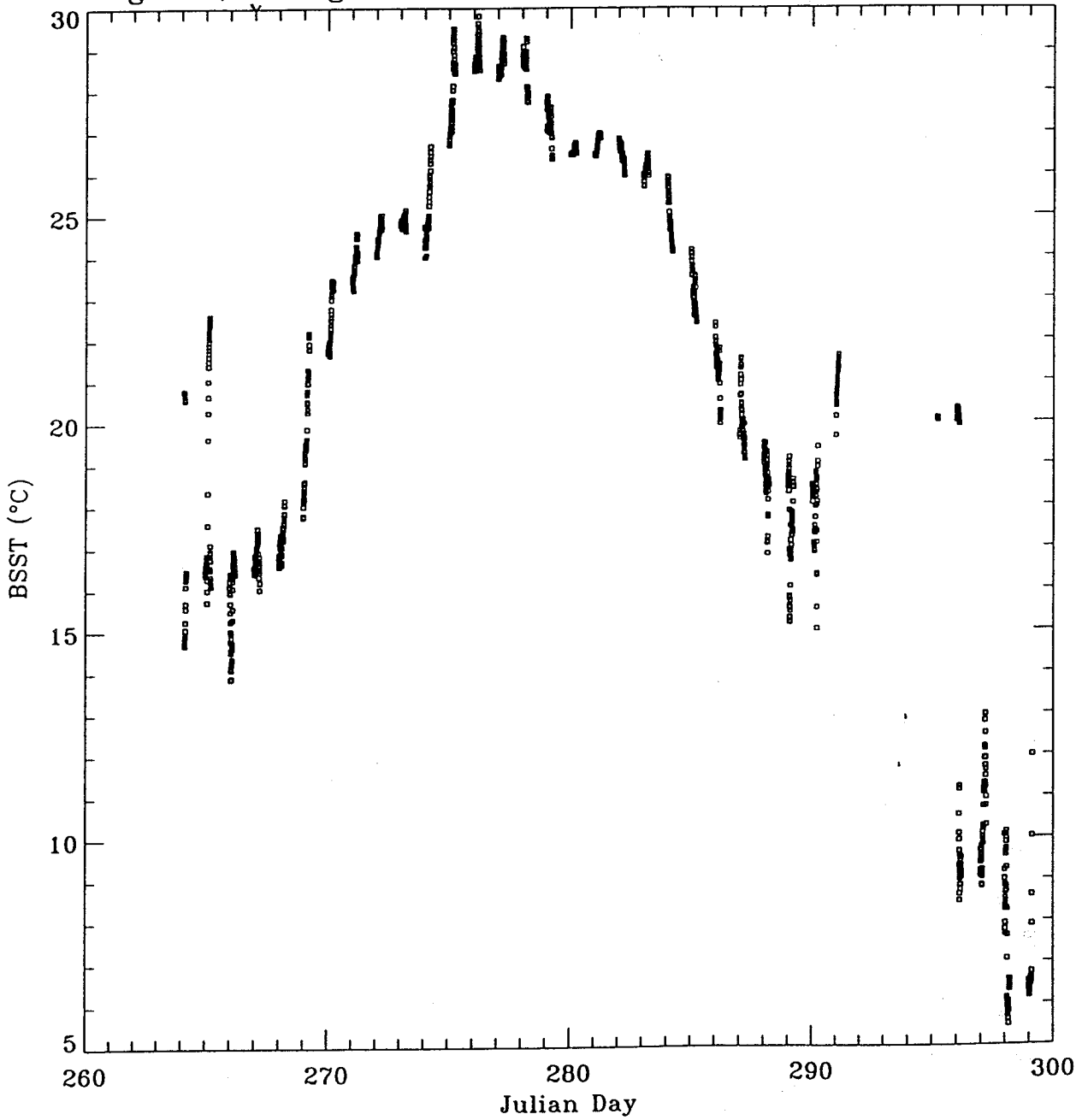

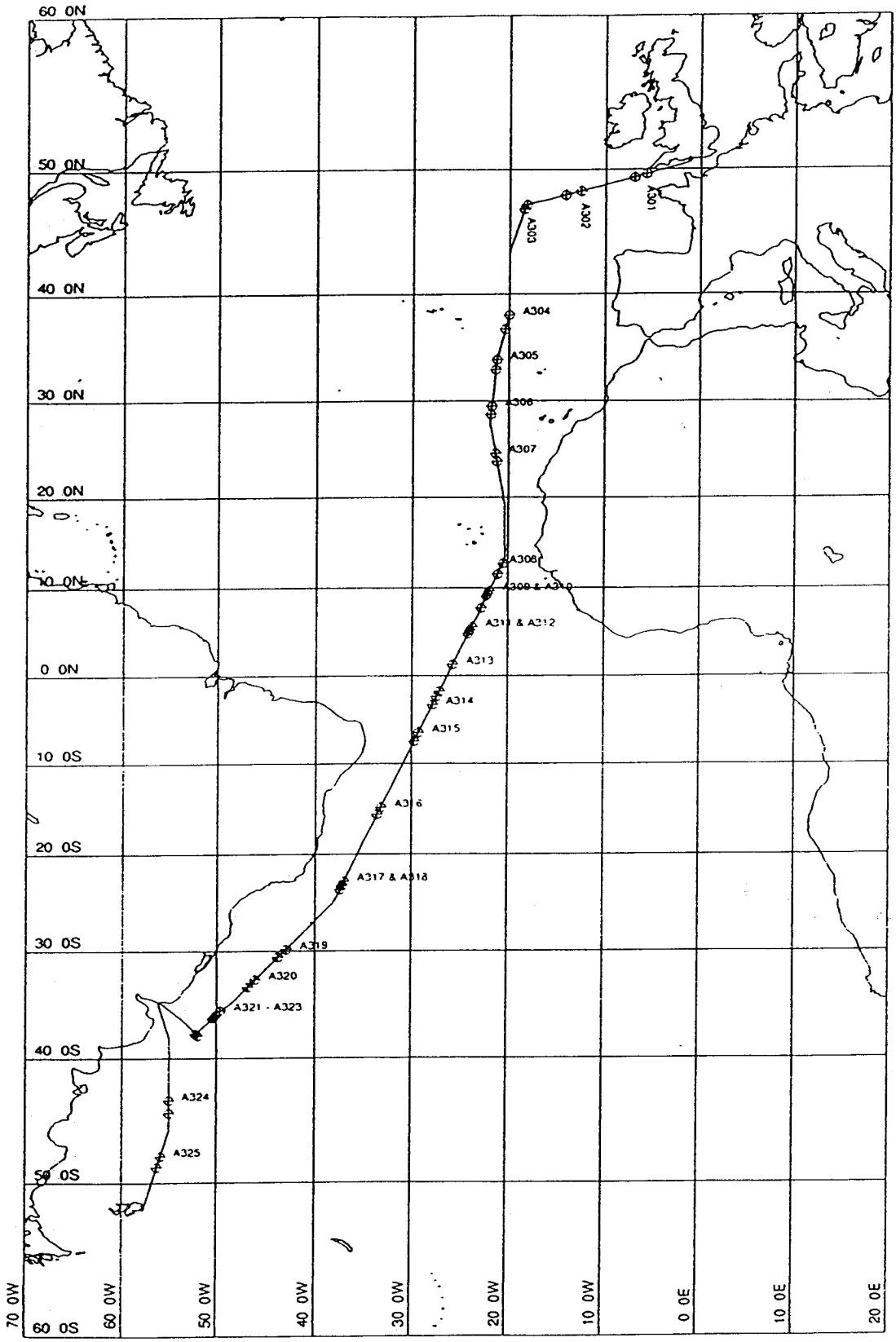

MERCATOR PROJECTION

SCALE : TC 5566:934 (NATURAL SCALE AT LAT -0)

INTERNATIONAL SPHEROID PROJECTED AT LATITUDE -0

GRID NO 1

Figure 10

Ship's track showing UOR deployment during AMT3

Figure 11 Range of wind speeds encountered during ROSSA 1996

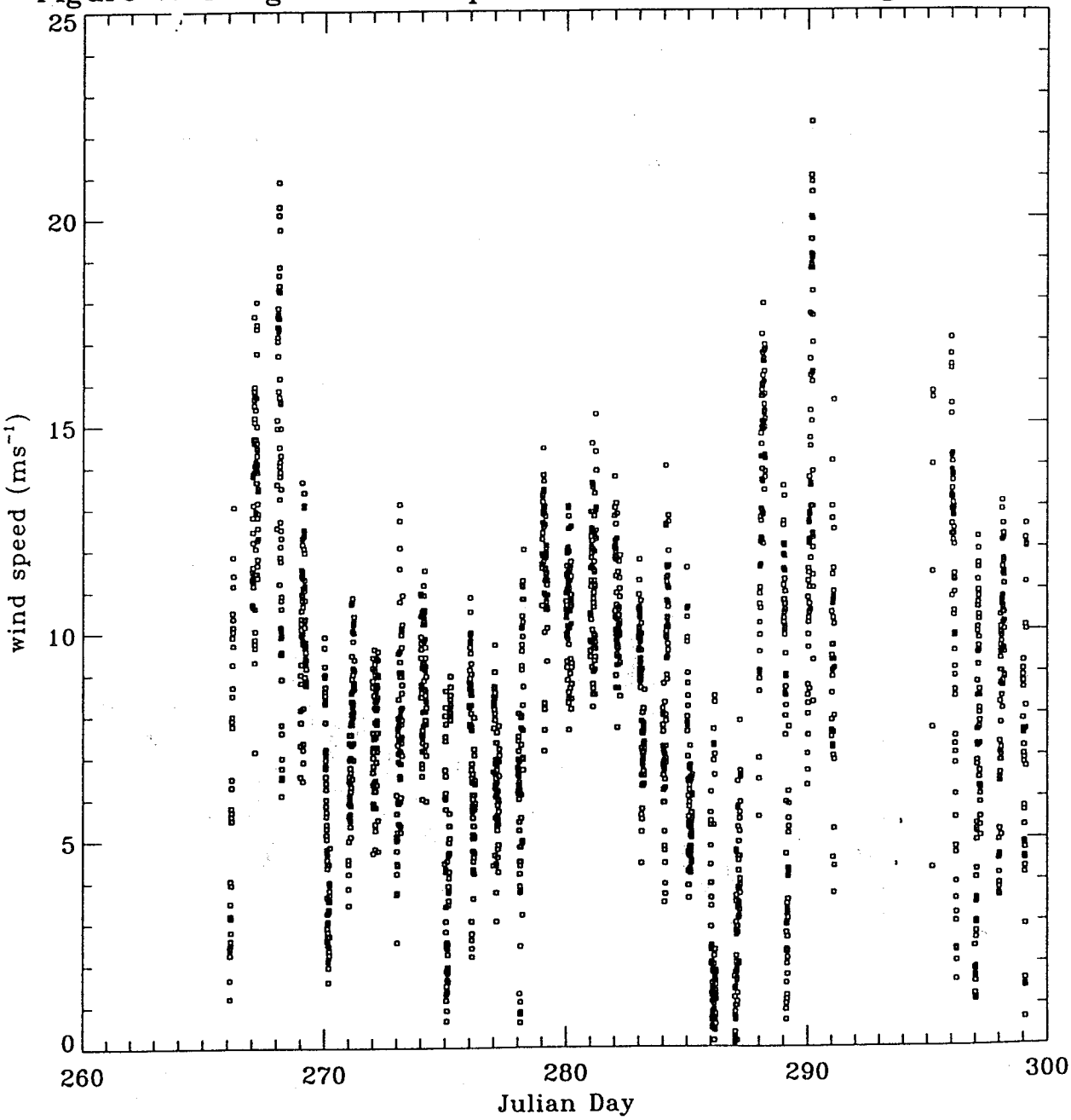

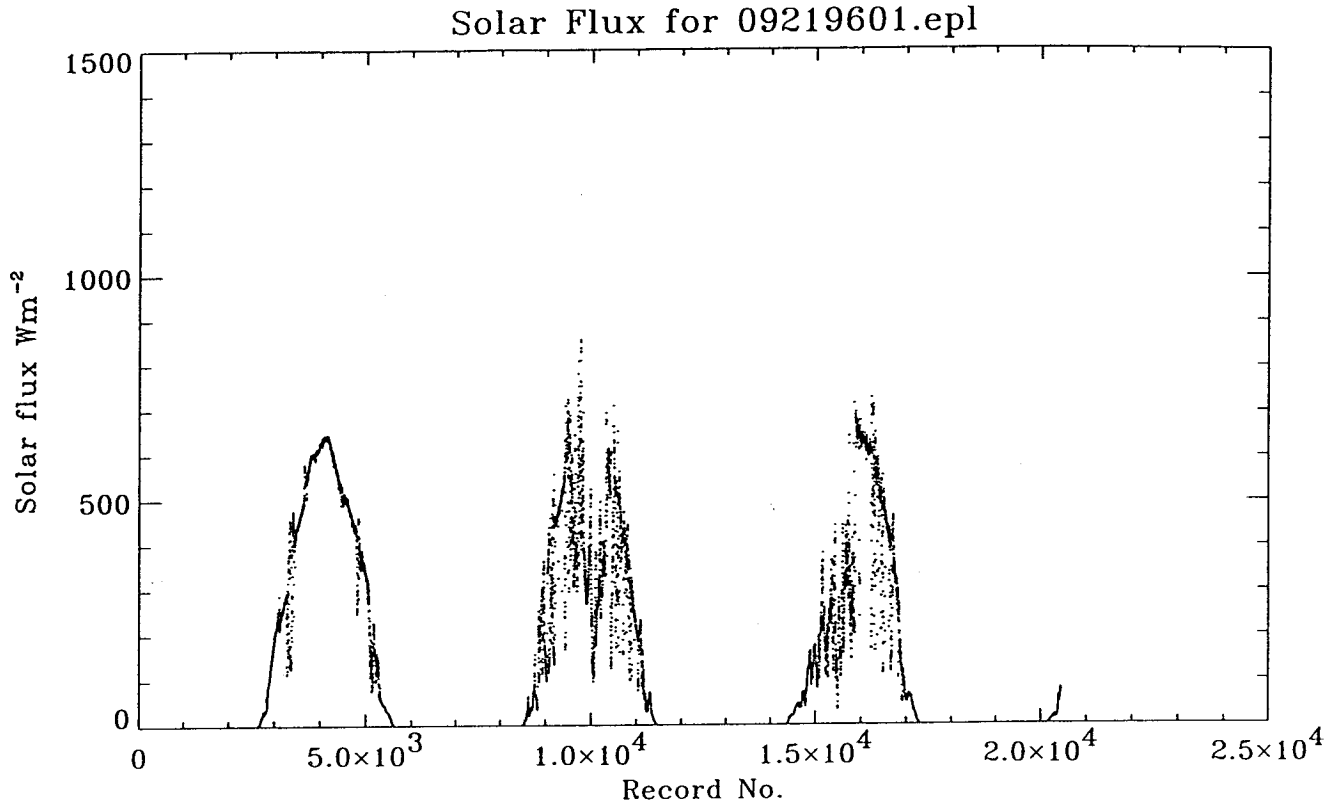
Solar Flux for 09219601.epl
Solar flux Wm^{-2}
1500
1000
500
0
0
5.0×10^3
1.0×10^4
1.5×10^4
2.0×10^4
2.5×10^4
Record No.

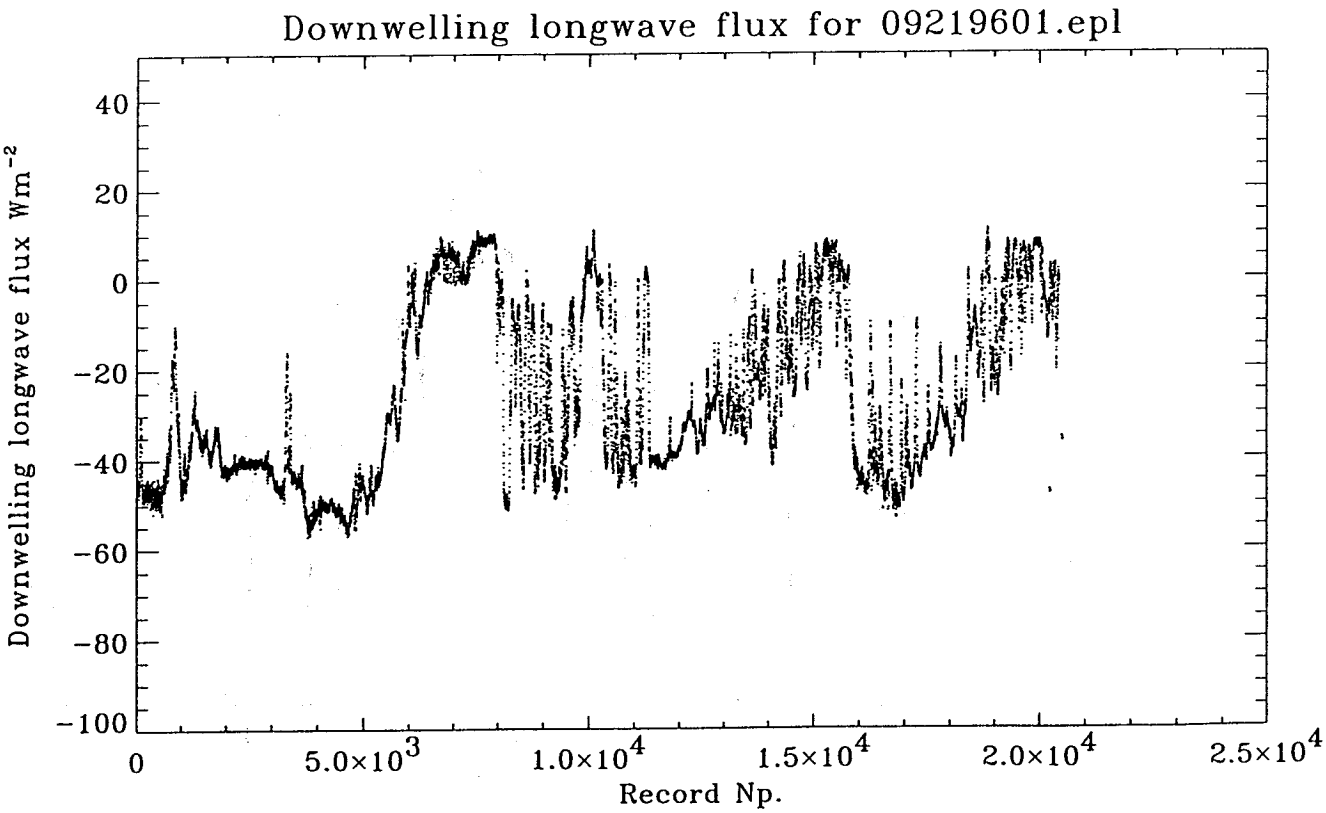
Downwelling longwave flux for 09219601.epl
Downwelling longwave flux Wm^{-2}
40
20
0
−20
−40
−60
−80
−100
0
5.0×10^3
1.0×10^4
1.5×10^4
2.0×10^4
2.5×10^4
Record Np.

Figure 12

ROSSA 1996: Radiosonde release positions.
RRS James Clark Ross September – October 1996

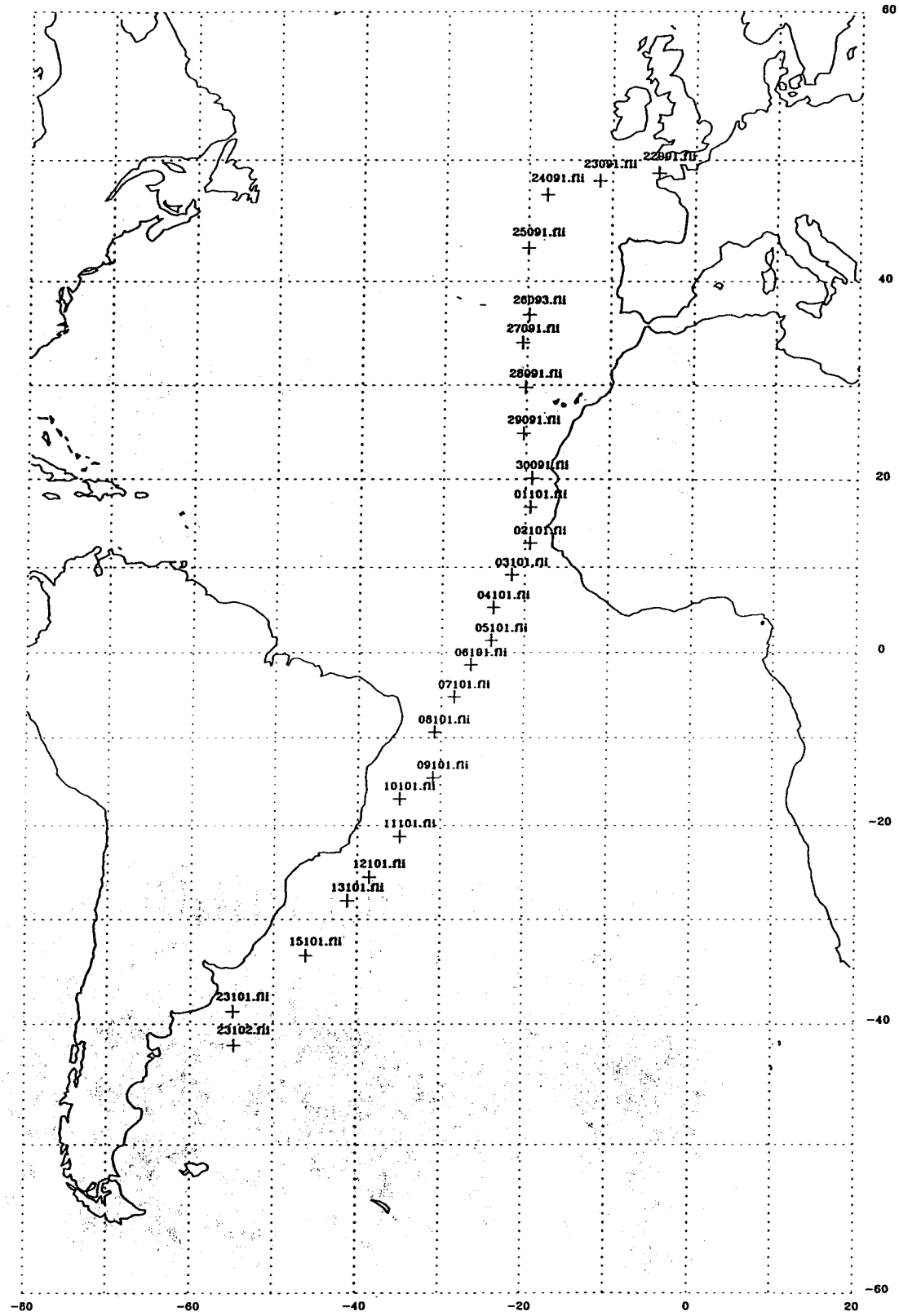

Figure 15

C J Donlon: RRS James Clark Ross, ROSSA September – October 1996.

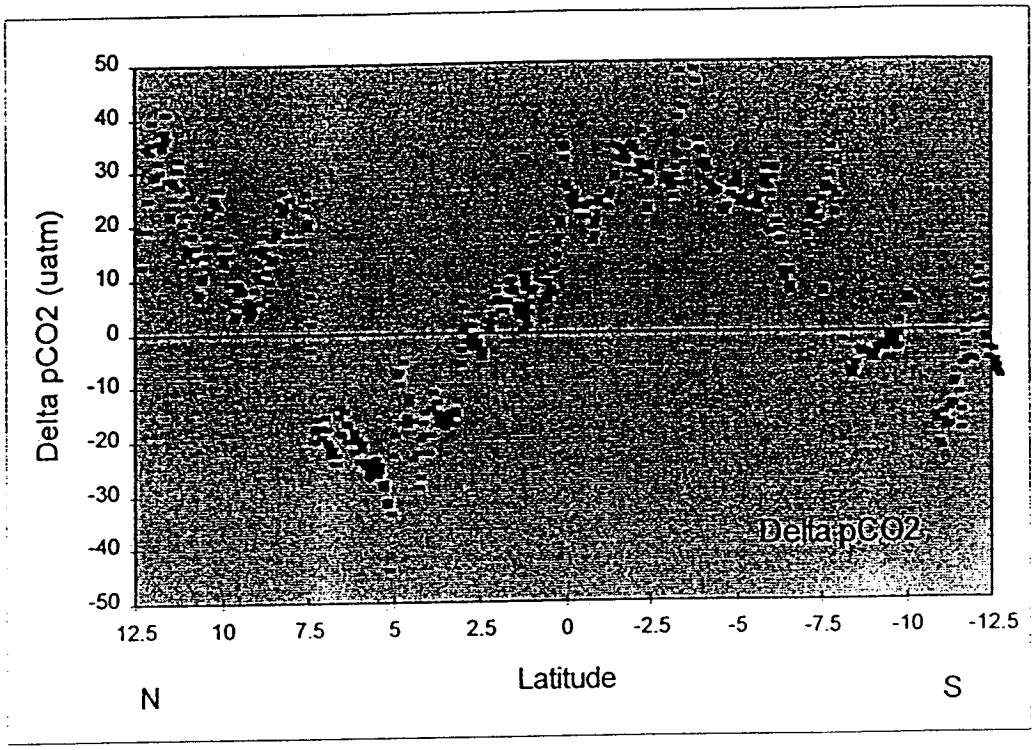
Delta pCO2 (uatm)
50
40
30
20
10
0
-10
-20
-30
-40
-50
Delta pCO2
12.5
10
7.5
5
2.5
0
-2.5
-5
-7.5
-10
-12.5
N
Latitude
S

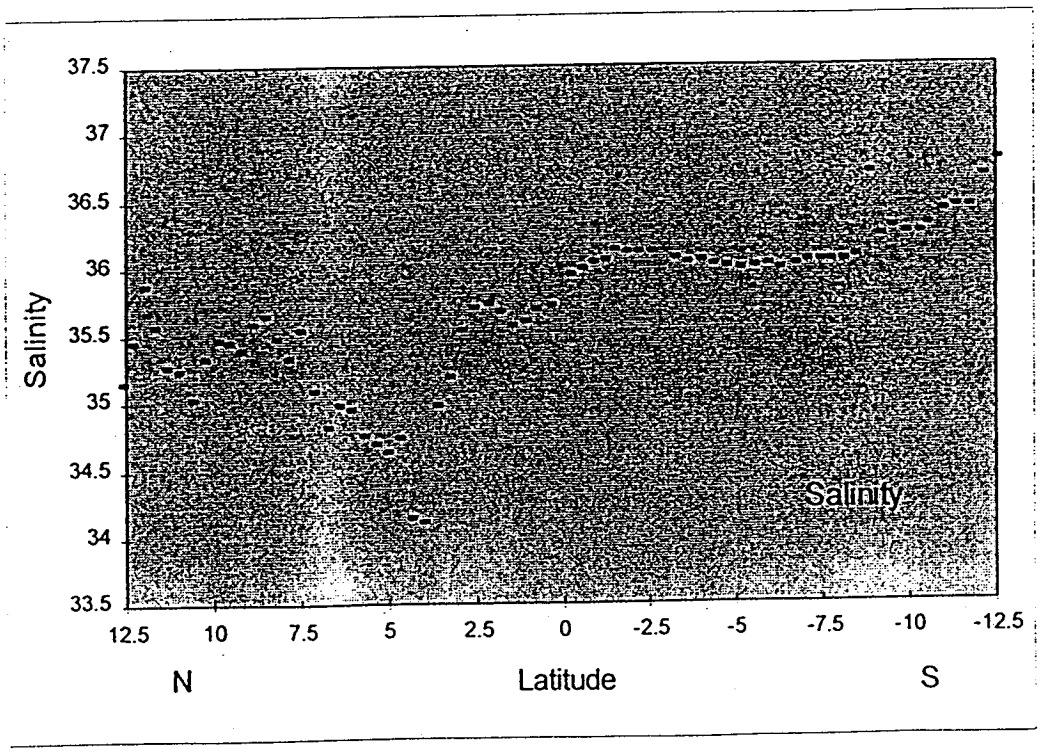
Salinity
37.5
37
36.5
36
35.5
35
34.5
34
33.5
Salinity
12.5
10
7.5
5
2.5
0
-2.5
-5
-7.5
-10
-12.5
N
Latitude
S

Figure 14